TN 1293

RECEIVED
10 JUN 1947
N.A.C.A. - W.D.
LOS ANGELES

NATIONAL ADVISORY COMMITTEE FOR AERONAUTICS

TECHNICAL NOTE

No. 1293

TESTS OF THE NACA 64_1A212 AIRFOIL SECTION WITH A SLAT, A DOUBLE SLOTTED FLAP, AND BOUNDARY-LAYER CONTROL BY SUCTION

By John H. Quinn, Jr.

Langley Memorial Aeronautical Laboratory
Langley Field, Va.

TECHNICAL LIBRARY
AIRESEARCH MANUFACTURING CO.
9851-9951 SEPULVEDA BLVD.
INGLEWOOD,
CALIFORNIA

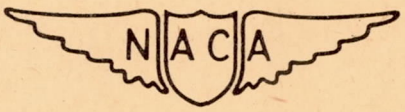

Washington
May 1947

NATIONAL ADVISORY COMMITTEE FOR AERONAUTICS

TECHNICAL NOTE NO. 1293

TESTS OF THE NACA 64_1A212 AIRFOIL SECTION WITH A SLAT, A DOUBLE SLOTTED FLAP, AND BOUNDARY-LAYER CONTROL BY SUCTION

By John H. Quinn, Jr.

SUMMARY

An investigation has been conducted of the NACA 64_1A212 airfoil section equipped with a leading-edge slat, a double slotted flap, and a boundary-layer-control suction slot at 0.40 chord to determine the maximum lift coefficients attainable with these high-lift devices alone and in conjunction with one another. The tests were made over a range of Reynolds number from 1.0×10^6 to 6.0×10^6 and included surveys to fine the optimum configurations for the slat and flap. The effects of boundary-layer suction on the maximum lift coefficient were determined for a range of flow coefficient C_Q from 0 to 0.03, where the flow coefficient is defined as the ratio of the quantity rate of air flow through the suction slot to the product of the wing area and free-stream velocity.

In general, the maximum section lift coefficient $c_{l_{max}}$ increased and the minimum section drag coefficient decreased with increasing flow coefficients. These changes were accompanied by small increases in the angle of attack for maximum lift and by small decreases in the angle of attack for zero lift. The results of the tests are summarized in the following table for a Reynolds number of 3.0×10^6:

Configuration	$c_{l_{max}}$		$\Delta c_{l_{max}}$
	$C_Q = 0$	$C_Q = 0.03$	
Plain airfoil	1.49	1.77	0.28
Airfoil and slat	1.86	2.46	.60
Airfoil and flap	2.82	3.12	.30
Airfoil, slat, and flap	3.30	3.86	.56

For all combinations of high-lift devices tested, the decrease in maximum lift coefficient produced by leading-edge roughness at a Reynolds number of 6×10^6 and a flow coefficient of 0.025 was less than that caused by roughness on the corresponding configuration without boundary-layer control.

INTRODUCTION

Previous investigations (references 1 and 2) have been conducted using boundary-layer control by suction on relatively thick NACA 6-series airfoil sections in an effort to bring about increases in the maximum lift coefficient. Substantial increments in maximum lift appeared obtainable by the use of boundary-layer suction, although the ultimate value of the maximum lift coefficient appeared to be limited by separation from the airfoil leading edge. Increasing the camber from zero to an amount that gave a design lift coefficient of 0.4 increased the maximum lift coefficient but did not change the nature of the stall. It seemed reasonable that if further increases in the maximum lift were to be obtained with boundary-layer control on these 6-series airfoil sections, some means of preventing leading-edge separation must be incorporated. The leading-edge slat has become recognized as one of the most effective devices for delaying leading-edge separation.

Tests have been conducted, therefore, of the NACA 64_1A212 airfoil section with a leading-edge slat, a double slotted flap, and a single boundary-layer suction slot at 0.40 chord to determine the increase in maximum lift coefficient attainable with this combination of high-lift devices. The optimum slat and flap configurations were determined, and the characteristics of the airfoil were measured for the high-lift devices operating individually and in conjunction with one another over a Reynolds number range from 1.5×10^6 to 6.0×10^6 in the Langley two-dimensional low-turbulence tunnel and the Langley two-dimensional low-turbulence pressure tunnel. The suction slot was placed at 0.40 chord inasmuch as this location was believed to be near the optimum location in conjunction with the slat, because the slat could be relied upon to delay separation near the leading edge. A suction-slot location closer to the leading edge might have a more favorable effect on the maximum lift of the airfoil without the slat; therefore, a few tests were made at a Reynolds number of 1.0×10^6 in order to find the effect of suction-slot location on the characteristics of the plain airfoil.

SYMBOLS

c_l section lift coefficient

c_d section drag coefficient

b airfoil span, feet

c airfoil chord, feet

V_o free-stream velocity, feet per second

Q quantity of air removed through suction slot, cubic feet per second

C_Q flow coefficient $\left(\frac{Q}{V_o c b}\right)$

H_o free-stream total pressure, pounds per square foot

H_b total pressure inside wing duct, pounds per square foot

q_o free-stream dynamic pressure, pounds per square foot

C_P pressure coefficient $\left(\frac{H_o - H_b}{q_o}\right)$

x horizontal distance parallel to chord line, feet

y vertical distance perpendicular to chord line, feet

δ angular deflection with respect to chord line, degrees

α_o section angle of attack, degrees

R Reynolds number $\left(\frac{V_o c}{\nu}\right)$

ν kinematic coefficient of viscosity

Subscripts:

s slat

v vane

f flap

MODELS

The 2-foot-chord models used in the present investigation were built to the ordinates of the NACA 64_1A212 airfoil section as presented in table 1. The A in the airfoil designation indicates that the cusp associated with the regular 6-series airfoil has been removed. Models built of laminated mahogany were used for the preliminary tests at the low Reynolds number and a cast-aluminum model was used to extend the tests to the higher Reynolds numbers. After the tests of the plain airfoil at low Reynolds numbers were finished, the leading and trailing edges of the wooden model with the 0.40c suction slot were modified to accommodate the leading-edge slat and the double slotted flap. The cast-aluminum model, that also had the suction slot located at 0.40c, was fitted with interchangeable leading edges to permit tests of the airfoil either with the true leading edge or with the leading-edge slat. Ordinates for the airfoil leading edge modified to accommodate the slat and for the slat, vane, and flap are presented in tables 2, 3, 4, and 5, respectively. A photograph of the aluminum model with the boundary-layer suction slot, leading-edge slat, and double slotted flap is presented as figure 1, and sketches of the model are presented as figure 2.

TESTS

The tests were conducted in the Langley two-dimensional low-turbulence tunnel (designated herein as LTT) and in the Langley two-dimensional low-turbulence pressure tunnel (designated herein as TDT). These tunnels have test sections 3 feet wide and $7\frac{1}{2}$ feet high and were designed to test models completely spanning the 3-foot jet in two-dimensional flow at a turbulence level approximately the same as that of free air. The LTT operates at atmospheric pressure. In the TDT the air may be compressed to a maximum value of 150 pounds per square inch absolute; therefore tests may be conducted at high Reynolds numbers and low Mach numbers. In both these tunnels lifts are obtained by integrating the pressure reactions along the floor and ceiling of the tunnel test section, and drags are obtained by the wake-survey method. The tunnels and methods of measurement are completely described in reference 3.

The air removed from the boundary layer was led through the suction slot into a duct inside the wing. The quantity of air removed was determined by means of a Venturi tube located in the pipe line between the airfoil and the blower used to force air flow

through the system. The total pressure inside the wing duct was obtained by a flush pressure orifice in the wing duct on the end opposite that at which the air was removed. For the no-flow condition, referred to as a flow coefficient of zero, the suction slot was filled and faired over with plasteline.

Tests were made at a Reynolds number of 1.0×10^6 in the LTT to find the effect of suction-slot location on the characteristics of the plain airfoil. The wooden model with the suction slot at 0.40c was then modified to permit surveys to find the optimum locations of the slat, vane, and flap at Reynolds numbers of 1.0×10^6 or 1.5×10^6. In making the slat surveys no intermediate supports were provided between the wing and slat, and fittings on the ends of the slat for changing the slat position and deflection were recessed in the tunnel end plates so that no disturbances in the flow were created near the airfoil leading edge.

Once the optimum configurations of the flap and slat were determined, the tests were extended to Reynolds numbers of 3.0×10^6 and 6.0×10^6 in the TDT with the aluminum model. For these tests the slat was attached to the airfoil by four struts, one at each end of the model and one 8 inches from each side of the model center line. Two small struts were also provided to brace the vane to the flap.

Some tests were conducted with 0.011-inch carborundum grains applied to the airfoil leading edge to find the effects of leading-edge roughness on the aerodynamic characteristics of the airfoil. The grains were applied with shellac over an area of the airfoil surface having a surface length of 0.08c from the leading edge on both surfaces so that 5 to 10 percent of this area was covered. For roughness applied in the slat-extended conditions the entire slat surface was roughened in addition to the roughness on the airfoil leading edge.

RESULTS AND DISCUSSION

Effect of Suction-Slot Location on Characteristics of Plain Airfoil

The effect of suction-slot location on the variation of the maximum lift coefficient and the minimum drag coefficient with the flow coefficient are presented in figure 3 for the plain airfoil section at a Reynolds number of 1.0×10^6. It was found that

both the maximum lift coefficient and the minimum drag coefficient increased as the suction slot was moved toward the leading edge. At a flow coefficient of 0.035, the model with the suction slot at 0.20c gave a maximum lift coefficient of 1.72, or approximately 0.16 greater than that for the slot at 0.40c. Inasmuch as tuft studies indicated that the air flow first separated at approximately 0.1c, it seems logical that the suction slot at 0.20c would produce a greater effect on the maximum lift than the suction slot at 0.40c would because the slot at 0.20c would be closer to the point where separation first occurred. In addition, for a given flow rate, a larger part of the boundary layer is removed when the suction slot is closer to the leading edge where the boundary layer is thin. This fact would also tend to bring about larger increases in the maximum lift as the suction slot was moved forward. The increase in minimum drag coefficient with forward movement of the suction slot is attributed to the increasing distance behind the slot over which the boundary layer can develop.

Plain Airfoil Characteristics

Lift and drag characteristics of the NACA 64_1A212 airfoil section with the boundary-layer suction slot at 0.40c operating and with the slot sealed and faired are presented in figure 4 at a Reynolds number of 1.0×10^6 for the model in both the smooth and rough conditions. The maximum lift coefficients increased steadily as the flow coefficient increased. This increase was accompanied by small increases in the angle of attack for maximum lift and small decreases in the angle of zero lift. The decrease in angle of zero lift is attributed to thinner boundary layers over the rear part of the airfoil which produce an effect similar to that of increased airfoil camber. Increasing the flow coefficient from 0 to 0.03 increased the maximum lift coefficient from 1.09 to 1.50 for the smooth airfoil and from 1.07 to 1.44 for the rough airfoil. The maximum lift coefficient was found from tuft observations to be limited by stalling at the leading edge. For the smooth condition at a flow coefficient of 0.02 and at an angle of attack of 10°, a small region of separated flow was observed at approximately 0.1c although from the suction slot to the trailing edge the flow adhered to the surface. At an angle of attack of 11°, intermittent separation occurred between the leading edge and the suction slot with unsteady flow from the slot to the trailing edge. At 12°, the angle of attack for maximum lift, the flow was completely separated between the leading edge and approximately 0.1c, with unsteady flow to the trailing edge. Observations of the wing with leading-edge roughness showed that the stall progression was similar to that for the wing in the smooth condition.

The effect of boundary-layer control on the drag characteristics was to decrease the minimum profile-drag coefficient as the flow coefficient increased and to maintain low drag coefficients to rather large lift coefficients.

The lift and drag characteristics for the airfoil with boundary-layer control at Reynolds numbers of both 3.0×10^6 and 6.0×10^6 are presented in figures 5 and 6, respectively. The effects of boundary-layer control are similar to those described for a Reynolds number of 1.0×10^6. The pressure coefficient C_p is presented as a function of section angle of attack. The drag coefficient equivalent to the power required to discharge the air removed from the boundary layer at free-stream total pressure may be obtained as the product of the pressure coefficient and the flow coefficient at any lift coefficient. This drag coefficient added to the corresponding profile-drag coefficient is the total drag of the airfoil with boundary-layer control. The horsepower required for boundary-layer control may be calculated for any given condition from the expression

$$\text{Horsepower} = \frac{Q(H_o - H_b)}{550}$$

The values for Q and $(H_o - H_b)$ may be obtained by multiplying C_Q and C_p by the applicable values of wing area, airplane velocity, and dynamic pressure.

The effects of Reynolds number and leading-edge roughness on the variation of maximum lift coefficient and minimum drag coefficient with flow coefficient for the plain airfoil are presented in figure 7. For the smooth condition, large increases in maximum lift throughout the range of flow coefficient were obtained by increasing the Reynolds number from 1.0×10^6 to 3.0×10^6. This favorable scale effect may be due to improved flow conditions about the airfoil leading edge at the higher Reynolds number. Almost no further increase in maximum lift was obtained by increasing the Reynolds number from 3.0×10^6 to 6.0×10^6. The greatest maximum lift coefficient measured was 1.77 at a flow coefficient of 0.03 and a Reynolds number of 3.0×10^6. This lift coefficient was 0.28 greater than that of the airfoil with no boundary-layer control at the same Reynolds number. Leading-edge roughness had almost no effect on the maximum lift coefficient of the airfoil at a Reynolds number of 1.0×10^6, but at a Reynolds number of 6.0×10^6 it decreased the maximum lift coefficient from 1.50 to 1.13 at a flow coefficient of 0 and from 1.75 to 1.44 at a flow coefficient of 0.025. For the rough condition little scale effect was found between Reynolds numbers of 1.0×10^6 and 6.0×10^6.

An appreciable decrease in the minimum drag coefficient was obtained by increasing the Reynolds number from 1.0×10^6 to 3.0×10^6, and little further decrease was obtained between 3.0×10^6 and 6.0×10^6. Leading-edge roughness produced large increases in the minimum drag coefficient without boundary-layer control at Reynolds numbers of both 1.0×10^6 and 6.0×10^6. At a flow coefficient of 0.03 and a Reynolds number of 1.0×10^6, the drag coefficients were approximately equal for the smooth and the rough conditions. At a Reynolds number of 6.0×10^6, the minimum drag coefficient was greater for the rough condition than for the smooth condition for all flow coefficients investigated.

Effect of Irregularities Caused by Slat Installation

A slat having a rounded leading edge would produce somewhat greater maximum lift increments than one with the sharp edge necessary to make the slat fair smoothly into the airfoil contour. (See reference 4.) A round leading-edge slat was accordingly selected for present tests and the effect on the lift and drag characteristics of the discontinuity at the lower surface of the airfoil with the slat retracted was evaluated at a Reynolds number of 1.5×10^6. The results are presented in figure 8. The sole effect of the discontinuity on the lift characteristics comprised a reduction in maximum lift coefficient from 1.21 to 1.16. Somewhat larger effects were found on the variation of drag coefficient with lift coefficient. The discontinuity generally produced rather large drag increments at low lift coefficients by increasing the drag coefficient from 0.0060 to 0.0105 at a lift coefficient of 0.2. As the lift coefficient increased, however, the effect of the discontinuity became smaller and at a lift coefficient of 0.6 it increased the drag coefficient by only 0.0015. In practice, therefore, some provision should be made to fair over the discontinuity.

Characteristics of Airfoil with Slat Extended

The results of the surveys to find the optimum position of the leading-edge slat with respect to the airfoil leading edge are presented in figure 9 for a Reynolds number of 1.0×10^6 and a flow coefficient of approximately 0.03. Little difference in the maximum lift coefficient attainable with the slat and boundary-layer control was found within the range of slat deflection between 18.2° and 28.3°. A slat deflection of 22.0° gave a value of the maximum lift coefficient of approximately 2.78 as compared with values of 2.70 and 2.74 for the 18.2° and 28.3° deflections, respectively. The maximum-lift contours presented in figure 9(b) show that maximum lift coefficient increased rather slowly as the

slat was moved forward of the airfoil leading edge until a maximum value was reached, at which point the lift dropped rapidly for further forward movement of the slat. As the slat angle was increased the optimum location of the slat with respect to the airfoil changed in such a way that the trailing edge of the slat moved down toward the airfoil chord.

Observations of the stall progression by means of tufts indicated that the stalling characteristics of the airfoil varied considerably with slat deflection. At a deflection of 18.2°, the maximum lift coefficient was limited by stalling on the slat followed by separation from the airfoil leading edge. At a slat deflection of 22.0°, the slat and airfoil appeared to stall simultaneously, although the flow on the slat at high angles of attack was more unsteady than that on the wing. At a deflection of 28.3°, the slat was not observed to stall, but separation again occurred at the airfoil leading edge.

Because the slat at a deflection of 22.0° and a location of $x_s = 0.046c$, $y_s = 0.037c$ gave the highest value of the maximum lift coefficient, the lift and drag characteristics of this configuration were determined at a Reynolds number of 1.5×10^6 and the results are presented in figure 10. The maximum lift coefficient without boundary-layer control was only 0.93, or less than that of the plain airfoil section. At a flow coefficient of 0.01, two entirely different lift curves could be obtained, depending upon the testing sequence used in obtaining the data. A hysteresis effect on lift due to change in the flow coefficient existed such that if the flow coefficient was raised from 0 to 0.01 in starting the lift curve, the maximum lift coefficient was 1.15 and occurred at an angle of attack of 13°. If the flow coefficient was first increased to an approximate value of 0.02 and then reduced to 0.01 before beginning the curve, a maximum lift coefficient of 2.57 was obtained at an angle of attack of 26°. No such hysteresis was found at a flow coefficient of 0.02. The drag characteristics in figure 10(b) show that beginning at a lift coefficient of 0.3, the drag coefficient increased rapidly with the lift coefficient up to a lift coefficient of approximately 1.3, at which point the drag coefficient decreased very rapidly. Between lift coefficients of 0.3 and 1.3 the flow between the slat and the leading edge was thought to be very poor because of blanketing action of the leading-edge slat. At a lift coefficient of 1.3 the flow probably became smooth at the leading edge and, therefore, brought about large reductions in drag. The inconsistency of the lift results at a flow coefficient of 0.01 and the low maximum lift coefficient of the airfoil without boundary-layer control probably result from poor flow through the gap between the slat and the leading edge. Figure 9(b) shows that at a value of $x_s = 0.046c$ the slat was extremely close to the point where lift decreased rapidly with forward movements of the slat. Because of this

fact, and the uncertain lift characteristics at low flow coefficients, it was decided to fix the slat closer to the airfoil leading edge for further tests. The slat, therefore, was fixed at $x_s = 0.036c$, $y_s = 0.037c$ for a deflection of 22.0°. Results of tests of the slat in this position are presented in figure 11 for Reynolds numbers of 1.5×10^6, 3.0×10^6, and 6.0×10^6. A comparison of the results presented in figure 11(a) and those for the slat farther forward in figure 10(a) shows that moving the slat back toward the airfoil leading edge eliminated the uncertainties in the variation of the lift coefficient with the angle of attack at low flow coefficients, increased the maximum lift coefficient without boundary-layer control from 0.93 to 1.6, and caused slight decreases in the maximum lift coefficient with boundary-layer control. Results of tests at Reynolds numbers of 3.0×10^6 and 6.0×10^6 for the slat in its optimum position are presented in figures 11(b) and 11(c) for the model in the smooth condition and in figure 11(d) for the model with leading-edge roughness at a Reynolds number of 6.0×10^6. The maximum lift coefficients of 2.62, 2.46, and 2.26 were obtained in the smooth condition at flow coefficients of 0.030, 0.030, and 0.024 at Reynolds numbers of 1.5×10^6, 3.0×10^6, and 6.0×10^6, respectively. These data are summarized in figure 12 in which the effect of Reynolds number on the variation of the maximum section lift coefficient with the flow coefficient is presented for the airfoil with the leading-edge slat. Without boundary-layer control the maximum lift coefficient was found to increase as the Reynolds number increased, although at flow coefficients above 0.01 the maximum lift coefficient was found to decrease as the Reynolds number increased. Inasmuch as the optimum position of the leading-edge slat was determined at a Reynolds number of 1.5×10^6, it is likely that the adverse effects of Reynolds number are due to changes in the nature of the flow that would alter the optimum slat position. For this reason, it would seem desirable to obtain optimum slat positions at Reynolds numbers as close as possible to those contemplated under flight conditions, although limitation of the test equipment prevented slat surveys at higher Reynolds numbers for the present series of tests. At a Reynolds number of 6.0×10^6 and at a flow coefficient of 0, roughness reduced the maximum lift coefficient from 1.94 to 1.42. At a flow coefficient of 0.025, however, boundary-layer control had offset the adverse effects of roughness and a maximum lift coefficient of 2.27 was obtained for the model both smooth and rough.

Characteristics of Airfoil with Double Slotted Flap

The results of the surveys to determine the optimum double-slotted-flap configuration are presented in figure 13 for a Reynolds number of 1.5×10^6. These surveys were made with the leading-edge

slat fixed in its optimum position and at a flow coefficient of 0.02. It was considered desirable to determine the optimum flap configurations in conjunction with the leading-edge slat inasmuch as preliminary measurements indicated that, without the slat, a large region of separated flow near the leading edge caused the maximum lift coefficient to be very insensitive to variations in the flap position. Little difference in the maximum lift coefficient attainable was found for the flap deflections of 49.7° and 55.0°, as shown in figures 13(a) and 13(b), respectively. A maximum lift coefficient of approximately 3.8 was obtained for a flap deflection of 55.0°. The maximum lift coefficient was found to be relatively insensitive to horizontal movements of the flap with respect to the vane, but was somewhat more sensitive to vertical movements. With the flap fixed with respect to the vane at the best locations found for a deflection of 55.0°, the vane and flap were moved as a unit to find the optimum positionfor the flap as a whole with respect to the airfoil section. The maximum lift contours for these surveys are shown in figure 13(c). It appeared that little further increases in the maximum lift could be obtained by moving the vane from its original position and that the maximum lift coefficient was quite sensitive to movements of the flap as a whole with respect to the wing. With the flap in the optimum position, random points were checked to determine whether the addition of the flap had altered the optimum position of the slat. The addition of the flap was found to produce little or no change in the optimum slat position.

The lift characteristics for the airfoil with the double slotted flap in its optimum position and with slat retracted at Reynolds numbers of 1.5×10^6, 3.0×10^6, and 6.0×10^6 are presented in figure 14. Figure 14(a) shows that little increase in the maximum lift coefficient was obtained with boundary-layer control at a Reynolds number of 1.5×10^6. The maximum lift coefficient for a flow coefficient of 0 was 2.48, and a flow coefficient of 0.02 brought about an increase in the maximum lift coefficient of only 0.14, which resulted in a maximum lift coefficient of 2.62. The relatively low maximum lift for a flow coefficient of 0 and the poor effectiveness of boundary-layer control are attributed to the large bubble of laminar separation occurring close to the airfoil leading edge. At Reynolds numbers of 3.0×10^6 and 6.0×10^6, however, as shown in figures 14(b) and 14(c), considerably higher maximum lift coefficients and greater increases with boundary-layer control were obtained. At a Reynolds number of 3.0×10^6 and a flow coefficient of 0.03, a maximum lift coefficient of 3.16 was obtained, as compared with a value of 2.82 with no suction. The improved characteristics of the airfoil at the higher Reynolds numbers are attributed to a decrease in the size of the separated-flow region near the leading edge. The effects of this bubble of separation are more fully discussed in reference 5. Data are presented in figure 14(d) for the model

with leading-edge roughness. The maximum lift coefficients were lower than the corresponding values for the smooth condition presented in figure 14(c), although rather large increases in maximum lift coefficient were obtained with increasing amount of boundary-layer control.

The data presented in figure 14 are summarized in figure 15 in which the effect of Reynolds number on the variation of maximum lift coefficient with flow coefficient is shown for the airfoil with the double slotted flap. Favorable scale effect was obtained throughout the ranges of flow coefficient and Reynolds number investigated. At a Reynolds number of 6.0×10^6, roughness reduced the maximum lift coefficient from 2.85 to 2.45 at a flow coefficient of 0, and from 3.23 to 2.86 at a flow coefficient of 0.025.

Characteristics of Airfoil with Leading-Edge Slat and Double Slotted Flap

Lift characteristics at Reynolds numbers of 1.5×10^6, 3.0×10^6, and 6.0×10^6 are presented in figure 16 for the model with the leading-edge slat and the double slotted flap with and without boundary-layer control. The characteristics of the airfoil with two high-lift devices (leading-edge slat and double slotted flap) in conjunction with boundary-layer control are similar to those of the airfoil alone or with only one other high-lift device with boundary-layer control. The greatest maximum lift coefficient obtained, 3.86, was found at a Reynolds number of 3.0×10^6 at a flow coefficient of 0.031 (fig. 16(b)).

The maximum lift characteristics for this configuration are summarized in figure 17. The maximum lift coefficients increased as the Reynolds number increased without boundary-layer suction. At flow coefficients above approximately 0.01, however, the maximum lift increased between Reynolds numbers of 1.5×10^6 and 3.0×10^6 and decreased between 3.0×10^6 and 6.0×10^6. Compared with the scale effect on the maximum lift characteristics of the airfoil with either the slat or flap alone (figs. 12 and 15), the effects of Reynolds number on the characteristics of this configuration were small. In the previous discussion of figures 12 and 15 it was observed that large favorable and unfavorable scale effects were encountered for the airfoil with boundary-layer control in conjunction with the double slotted flap and the leading-edge slat, respectively. When the two high-lift devices were combined, these diverse scale effects almost canceled each other. At a Reynolds number of 6.0×10^6, roughness decreased the maximum lift coefficient from 3.38 to 2.84 without boundary-layer control and from 3.72

to 3.40 at a flow coefficient of 0.025. As for the double slotted flap, a flow coefficient of 0.025 increased the maximum lift coefficient by an amount equal to the decrease caused by roughness without boundary-layer control.

Comparison of Maximum Lift Coefficients Obtained with Various High-Lift Devices

The maximum lift coefficients obtained with and without boundary-layer control at a Reynolds number of 3.0×10^6 are summarized for various combinations of high-lift devices in the following table:

Configuration	$c_{l_{max}}$		$\Delta c_{l_{max}}$
	$C_Q = 0$	$C_Q = 0.03$	
Airfoil	1.49	1.77	0.28
Airfoil and slat	1.86	2.46	.60
Airfoil and flap	2.82	3.12	.30
Airfoil, slat, and flap	3.30	3.86	.56

The addition of the leading-edge slat approximately doubled the increase in maximum lift coefficient obtainable with boundary-layer control.

The effects of leading-edge roughness on maximum lift coefficient for the airfoil with the various combinations of high-lift devices with and without boundary-layer control are summarized in the following table for a Reynolds number of 6.0×10^6:

Configuration	$C_Q = 0$			$C_Q = 0.025$		
	$c_{l_{max}}$		$\Delta c_{l_{max}}$	$c_{l_{max}}$		$\Delta c_{l_{max}}$
	Smooth	Rough		Smooth	Rough	
Airfoil	1.50	1.13	-0.37	1.75	1.44	-0.31
Airfoil and slat	1.94	1.42	-.52	2.27	2.27	0
Airfoil and flap	2.85	2.45	-.40	3.23	2.86	-.37
Airfoil, flap, and slat	3.38	2.84	-.54	3.72	3.40	-.32

The largest decrease in maximum lift coefficient due to roughness with boundary-layer control was no greater than the decrease produced by roughness on the plain airfoil section. For all combinations of high-lift devices tested the decrease in the maximum lift coefficient caused by roughness was less for the airfoil with boundary-layer control than for the corresponding configuration without boundary-layer control. For all combinations, a flow coefficient of 0.025 was sufficient to produce maximum lift coefficients on the roughened wing approximately equal to those obtained without boundary-layer control on the smooth wing.

SUMMARY OF RESULTS

The following statements summarize the results of the investigation of the NACA 64_1A212 airfoil section with a leading-edge slat, a double slotted flap, and boundary-layer control by suction to determine the maximum lift coefficients attainable over a Reynolds number range of 1.0×10^6 to 6.0×10^6:

1. In general, the maximum section lift coefficient was increased and the minimum section drag coefficient decreased by applying boundary-layer suction. These changes were accompanied by small increases in the angle of attack for maximum lift and by small decreases in the angle of attack for zero lift.

2. At a Reynolds number of 1.0×10^6, the maximum lift coefficient of the plain airfoil with boundary-layer control was limited by leading-edge separation. Increasing the Reynolds number to 3.0×10^6 produced rather large increases in maximum lift coefficient throughout the range of flow coefficient investigated. A maximum section lift coefficient of 1.77 was obtained at a Reynolds number of 3.0×10^6 and a flow coefficient of 0.03, which represented an increase in maximum lift coefficient of 0.28 over that of the airfoil without boundary-layer control.

3. With the leading-edge slat in its optimum position, increasing the flow coefficient from 0 to 0.030 increased the maximum lift coefficient from 1.86 to 2.46 at a Reynolds number of 3.0×10^6. Increasing the Reynolds number decreased the maximum lift coefficient attainable with the leading-edge slat. For this reason, it was thought that optimum slat positions for a given installation should be found at Reynolds numbers close to those at which the actual airplane would operate.

4. Increasing the flow coefficient from 0 to 0.030 with the double slotted flap increased the maximum lift coefficient

from 2.82 to 3.12 at a Reynolds number of 3.0×10^6. Increasing Reynolds number produced appreciable increases in maximum lift coefficient over the range of Reynolds number investigated.

5. The leading-edge slat and double slotted flap combined produced a maximum lift coefficient of 3.86 at a flow coefficient of 0.03 and a Reynolds number of 3.0×10^6 compared with a value of 3.30 at a flow coefficient of 0. Little scale effect was obtained with this combination.

6. For all combinations of high-lift devices tested, the decrease in maximum lift coefficient produced by roughness at a Reynolds number of 6.0×10^6 and a flow coefficient of 0.025 was less than that caused by roughness on the corresponding configuration without boundary-layer control.

Langley Memorial Aeronautical Laboratory
National Advisory Committee for Aeronautics
Langley Field, Va., March 19, 1947

REFERENCES

1. Quinn, John H., Jr.: Tests of the NACA 65_3-018 Airfoil Section with Boundary-Layer Control by Suction. NACA CB No. L4H10, 1944.

2. Quinn, John H., Jr.: Wind-Tunnel Investigation of Boundary-Layer Control by Suction on the NACA 65_3-418, a = 1.0 Airfoil Section with a 0.29-Airfoil-Chord Double Slotted Flap. NACA TN No. 1071, 1946.

3. von Doenhoff, Albert E., and Abbott, Frank T., Jr.: The Langley Two-Dimensional Low-Turbulence Pressure Tunnel. NACA TN No. 1283, 1947.

4. Weick, Fred E., and Platt, Robert C.: Wind-Tunnel Tests on Model Wing with Fowler Flap and Specially Developed Leading-Edge Slot. NACA TN No. 459, 1933.

5. Quinn, John H., Jr., and Tucker, Warren A.: Scale and Turbulence Effects on the Lift and Drag Characteristics of the NACA 65_3-418, a = 1.0 Airfoil Section. NACA ACR No. L4H11, 1944.

TABLE 1

NACA 64_1A212 AIRFOIL SECTION

(Stations and ordinates in percent airfoil chord)

Upper surface		Lower surface	
Station	Ordinate	Station	Ordinate
0	0	0	0
.409	1.013	.591	-.901
.648	1.233	.852	-1.075
1.135	1.580	1.365	-1.338
2.365	2.225	2.635	-1.803
4.849	3.145	5.151	-2.423
7.343	3.846	7.657	-2.874
9.842	4.432	10.158	-3.240
14.849	5.358	15.151	-3.796
19.862	6.060	20.138	-4.200
24.880	6.584	25.120	-4.482
29.900	6.956	30.100	-4.660
34.922	7.189	35.078	-4.741
39.946	7.272	40.054	-4.714
44.970	7.177	45.030	-4.549
49.993	6.935	50.007	-4.275
55.015	6.570	54.985	-3.918
60.034	6.103	59.966	-3.499
65.050	5.544	64.950	-3.034
70.064	4.903	69.936	-2.537
75.075	4.197	74.925	-2.037
80.090	3.433	79.910	-1.563
85.088	2.601	84.912	-1.159
90.062	1.751	89.938	-.771
95.032	.888	94.968	-.398
100.000	.025	99.999	-.025

L.E. radius: 0.994
Slope of radius through L.E.: 0.095

NATIONAL ADVISORY
COMMITTEE FOR AERONAUTICS

TABLE 2

MODIFIED LEADING EDGE OF NACA 64_1A212 AIRFOIL SECTION

(Stations and ordinates in percent airfoil chord)

Upper surface		Lower surface	
Station	Ordinate	Station	Ordinate
2.158	-0.833	2.167	-1.083
2.292	-.271	2.292	-1.417
2.500	.113	2.500	-1.625
2.917	.604	2.708	-1.767
3.333	.967	2.917	-1.871
4.167	1.471	3.333	-2.004
5.208	1.992		
6.250	2.438		
8.333	3.229		
10.417	4.000		
12.500	4.700		
14.000	5.142		

NATIONAL ADVISORY COMMITTEE FOR AERONAUTICS

TABLE 3

LEADING-EDGE SLAT FOR NACA 64_1A212 AIRFOIL SECTION

(Stations and ordinates in percent airfoil chord)

Upper surface		Lower surface	
Station	Ordinate	Station	Ordinate
0	0	1.458	-.783
.407	1.015	1.875	-.508
.646	1.234	2.083	-.292
1.132	1.582	2.708	.417
2.363	2.228	2.917	.625
4.846	3.151	3.333	.967
7.340	3.856	3.542	1.125
9.838	4.442	4.167	1.542
14.000	5.208	5.208	2.104
		6.250	2.604
		8.333	3.417
		10.417	4.167
		12.500	4.833
		14.000	5.142
L.E. radius: 0.994			
Slope of radius through L.E.: 0.097			

TABLE 4

VANE FOR NACA 64_1A212 AIRFOIL SECTION

(Stations and ordinates in percent airfoil chord)

Upper surface		Lower surface	
Station	Ordinate	Station	Ordinate
0	1.188	0	1.188
.100	1.585	.100	.813
.200	1.764	.200	.655
.596	2.198	.596	.317
.992	2.460	.992	.150
1.484	2.677	1.484	.029
1.981	2.794	1.981	0
2.477	2.836	2.477	.058
2.973	2.802	2.973	.179
3.465	2.744	3.465	.296
3.962	2.614	3.962	.438
4.458	2.435	4.458	.596
4.954	2.235	4.954	.742
5.446	2.000	5.446	.813
5.942	1.760	5.942	.834
6.438	1.484	6.438	.792
6.935	1.168	6.935	.676
7.427	.834	7.427	.475
7.923	.446	7.923	.200
8.240	.217	8 2 40	0
8.340	.138		

NATIONAL ADVISORY COMMITTEE FOR AERONAUTICS

TABLE 5

FLAP FOR NACA 64_1A212 AIRFOIL SECTION

(Stations and ordinates in percent airfoil chord)

Upper surface		Lower surface	
Station	Ordinate	Station	Ordinate
77.083	-.417	77.292	-1.042
77.292	.208	77.500	-1.208
77.708	.833	78.125	-1.458
78.125	1.250	79.167	-1.542
79.167	1.979	79.908	-1.546
80.208	2.458	84.910	-1.129
81.250	2.750	89.957	-.760
82.292	2.833	94.968	-.393
83.333	2.813	99.999	-.025
85.090	2.631		
90.063	1.762		
95.032	.892		
100.000	.025		

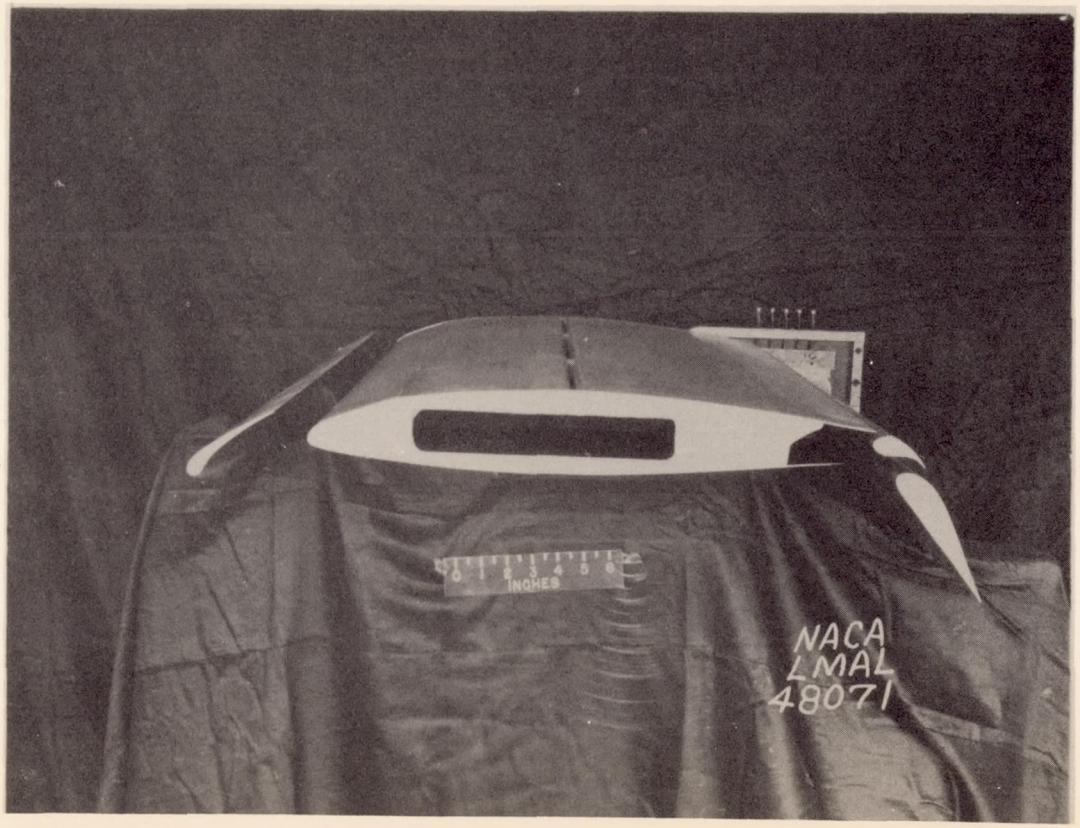

Figure 1.- NACA 64_1A212 airfoil section with boundary-layer suction slot, leading-edge slat, and double slotted flap.

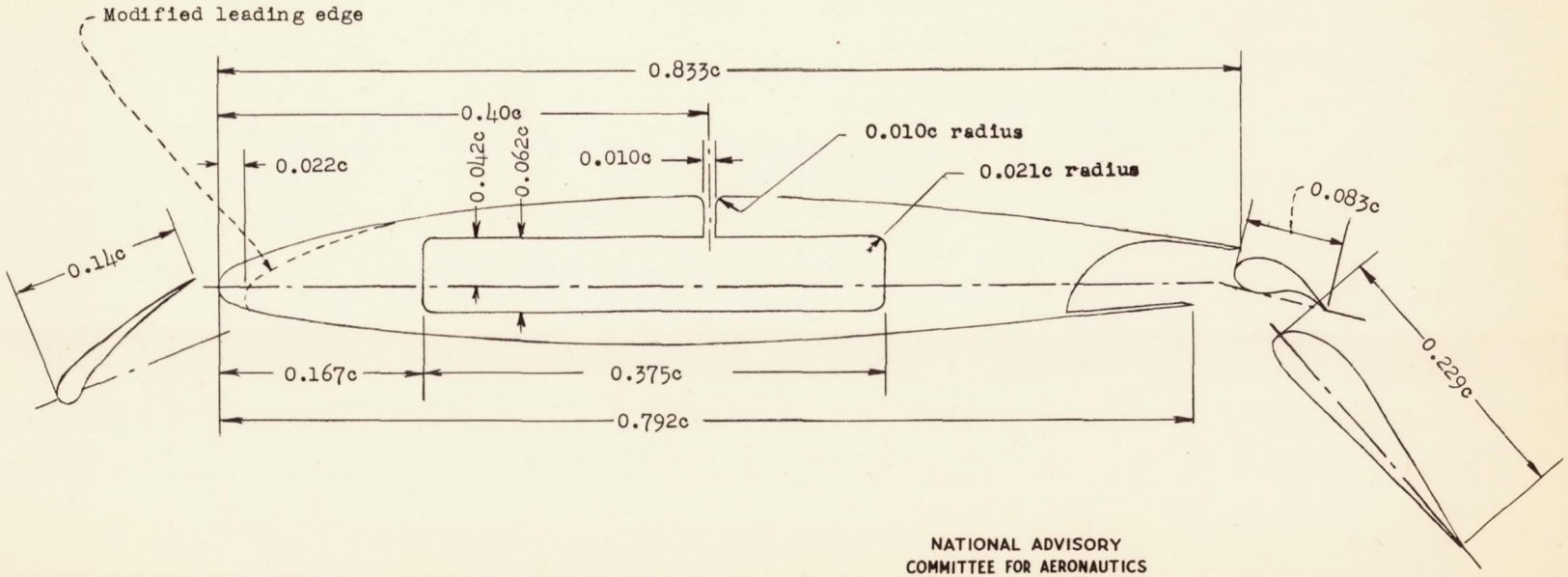

(a) Model dimensions.

Figure 2.- NACA 64_1A212 airfoil section with boundary-layer suction slot, leading-edge slat, and double slotted flap.

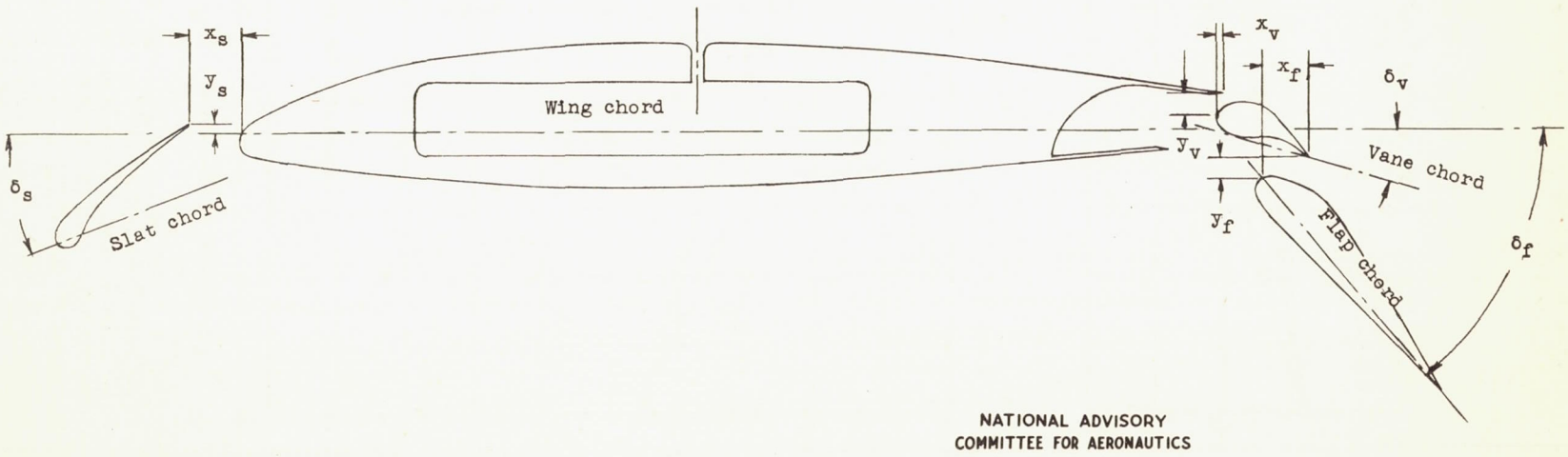

(b) Notation used to indicate positions of slat, vane, and flap.

Figure 2.- Concluded.

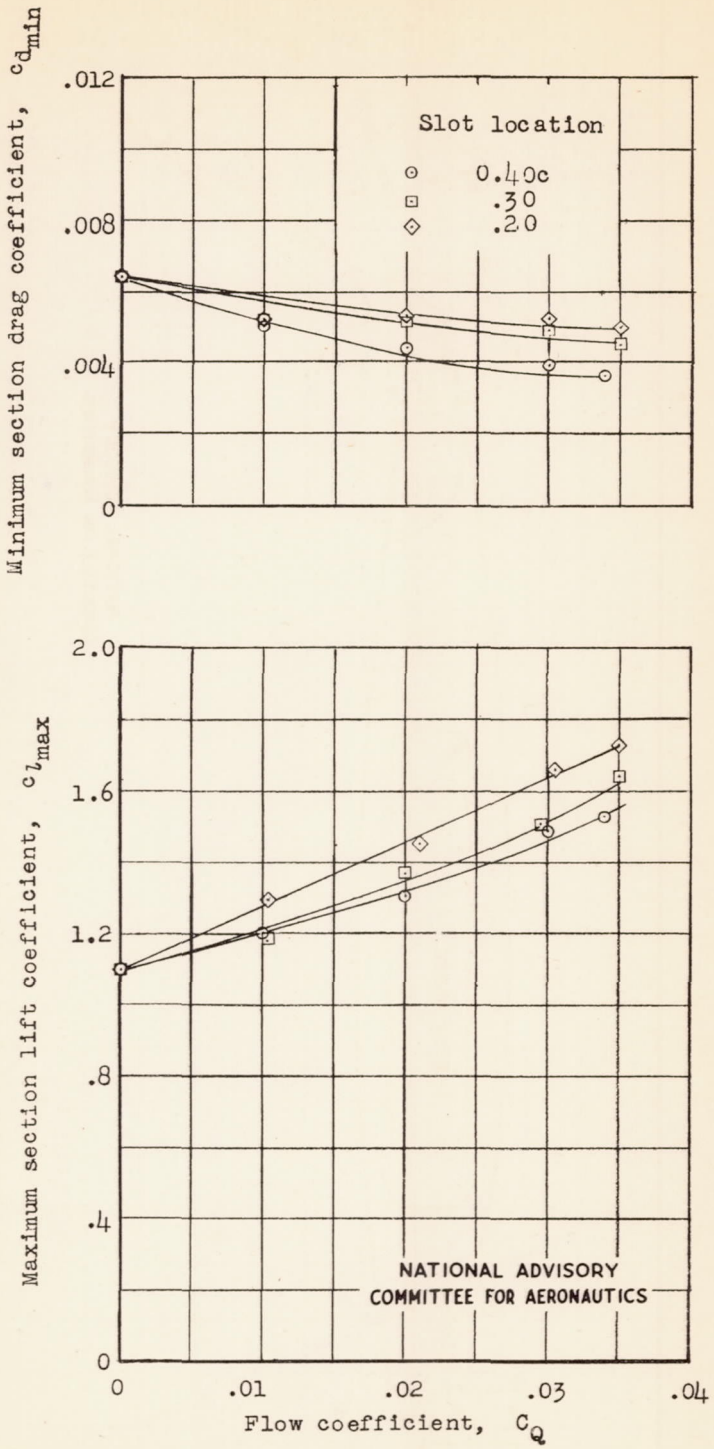

Figure 3.- Variation of maximum section lift coefficient and minimum section drag coefficient with flow coefficient for NACA 64_1A212 airfoil section with various boundary-layer suction-slot locations. R, 1.0×10^6.

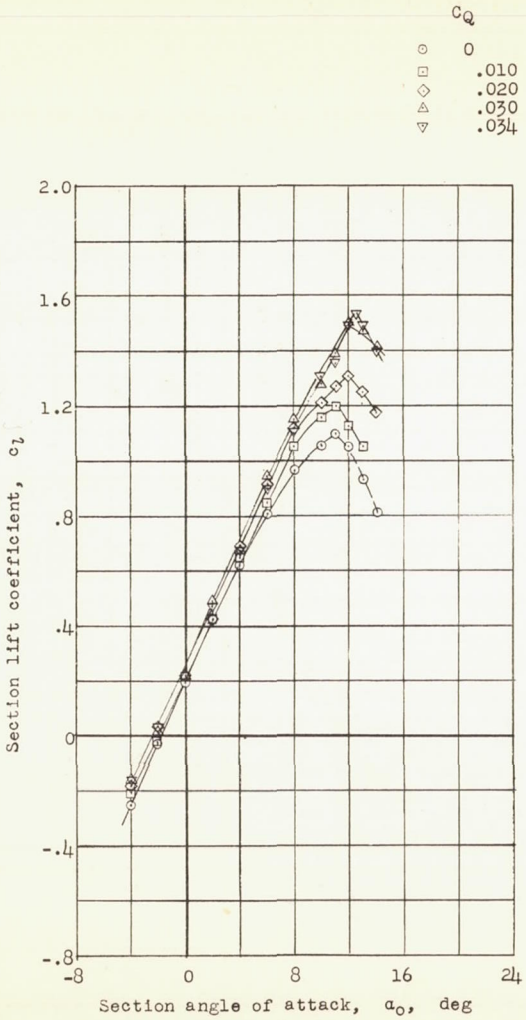

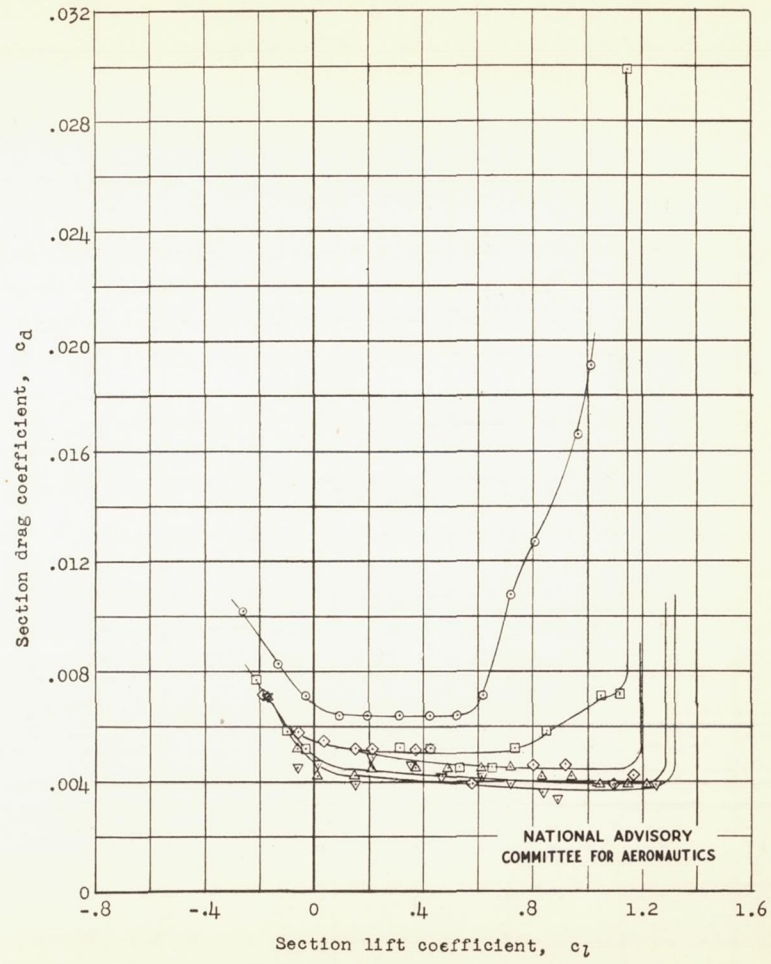

(a) Model in smooth condition.

Figure 4.- Lift and drag characteristics of NACA 64_1A212 airfoil section with boundary-layer control; suction slot at 0.40c. R, 1.0×10^6; tests, LTT 425, 426.

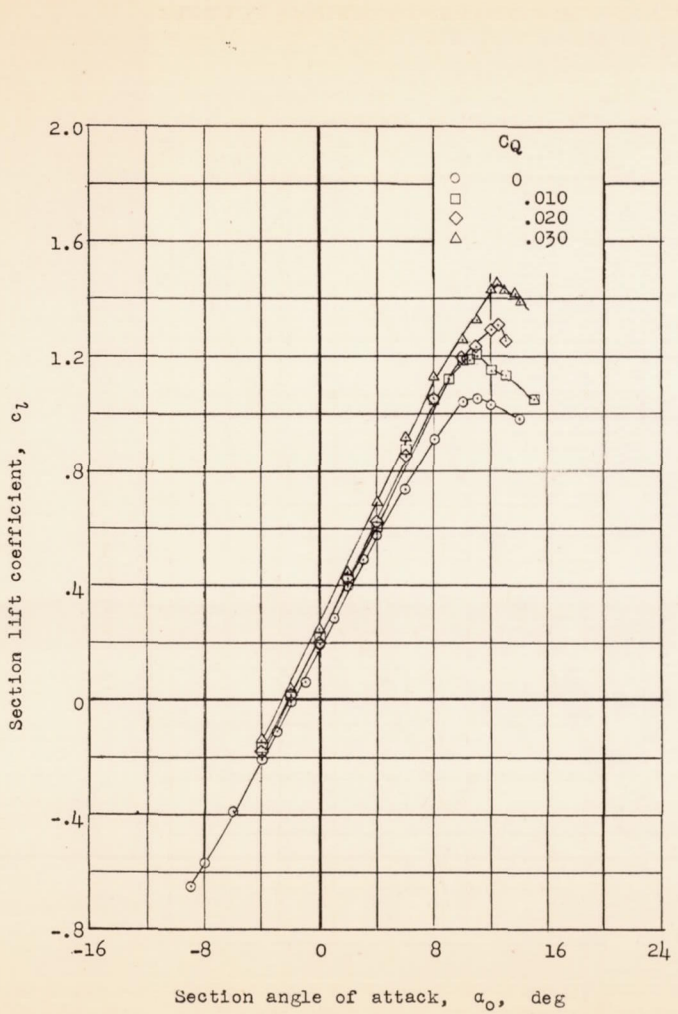

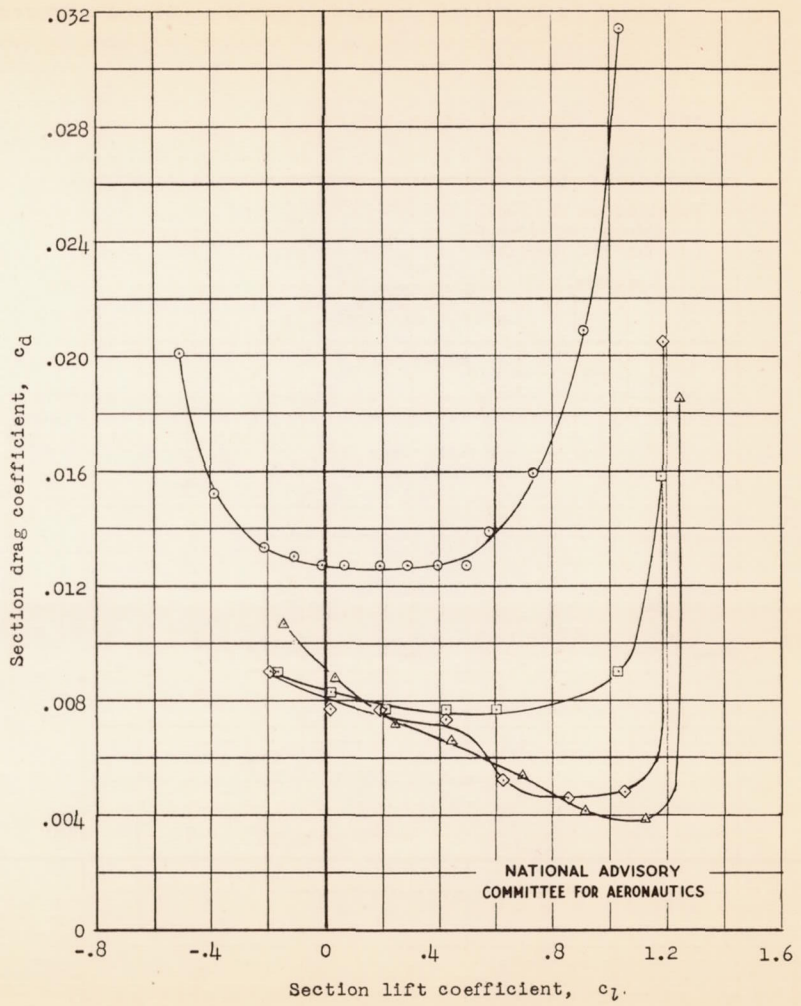

(b) Model with standard roughness.

Figure 4.- Concluded.

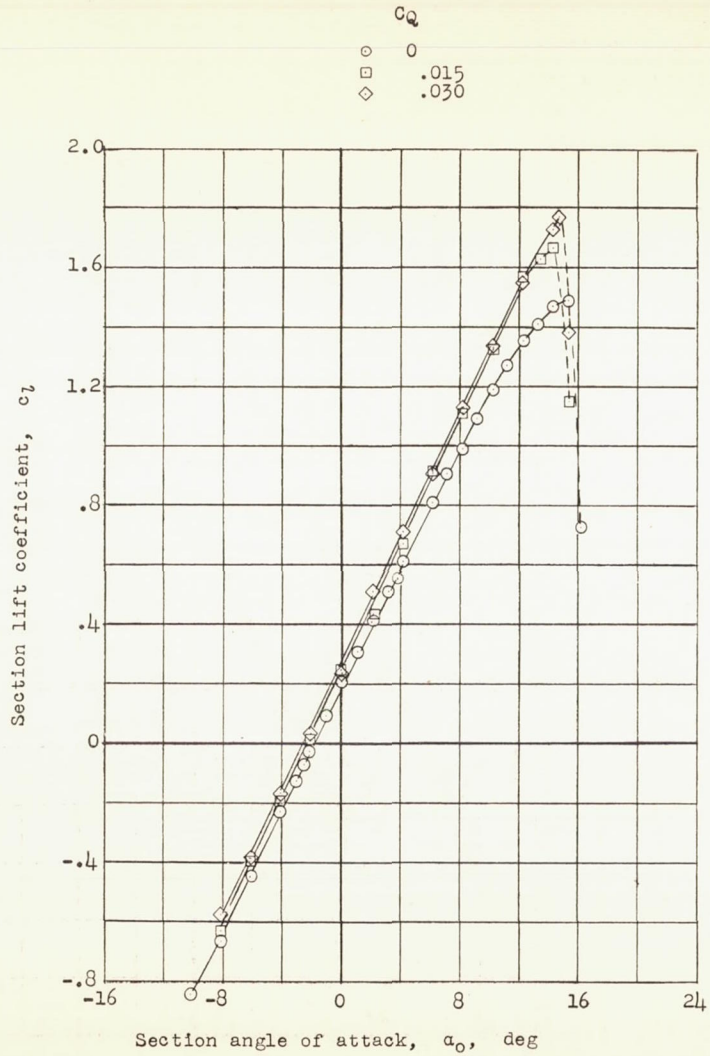

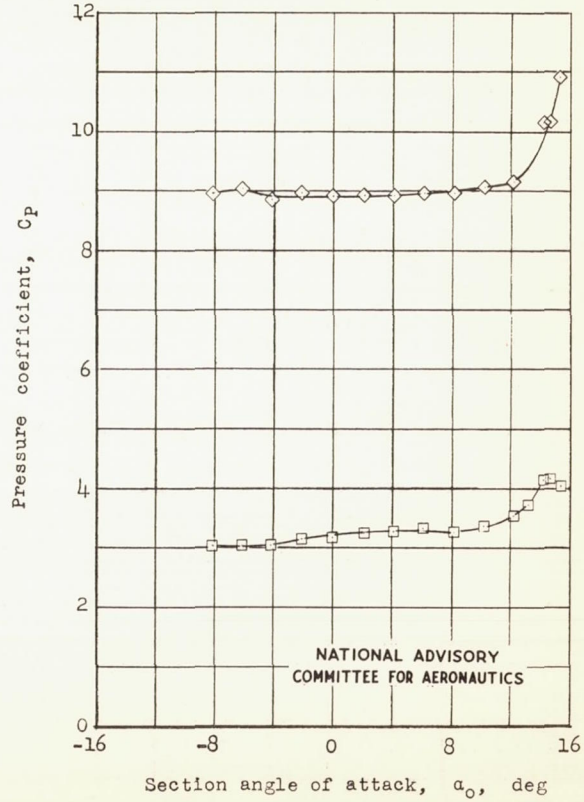

(a) $R = 3.0 \times 10^6$; model in smooth condition.

Figure 5.- Lift characteristics of NACA 64_1A212 airfoil section with boundary-layer control. Tests, TDT 953, 984.

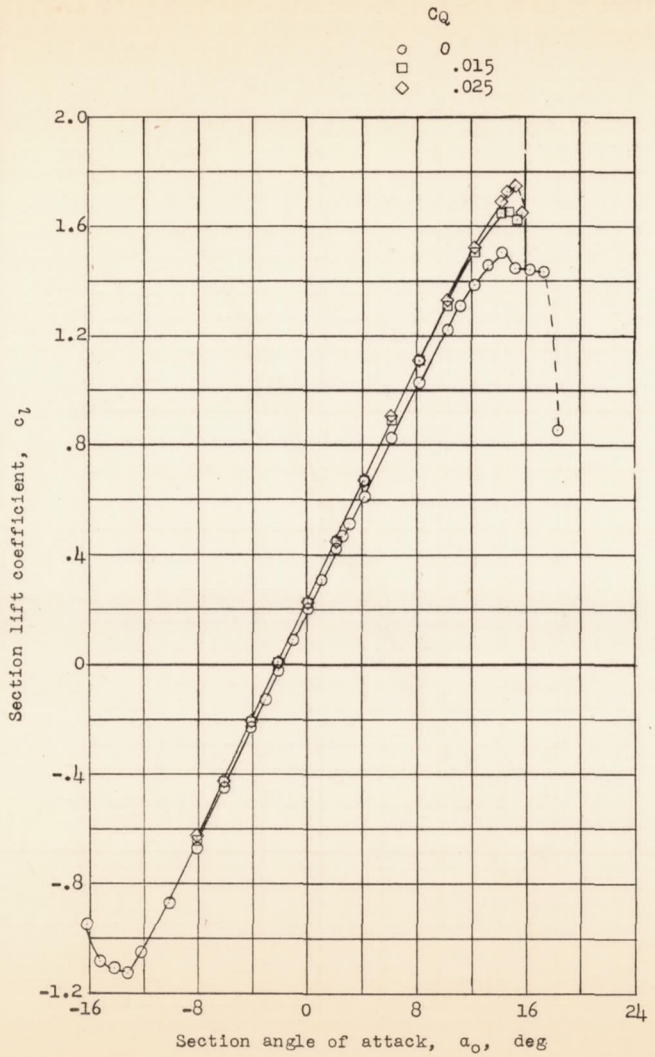

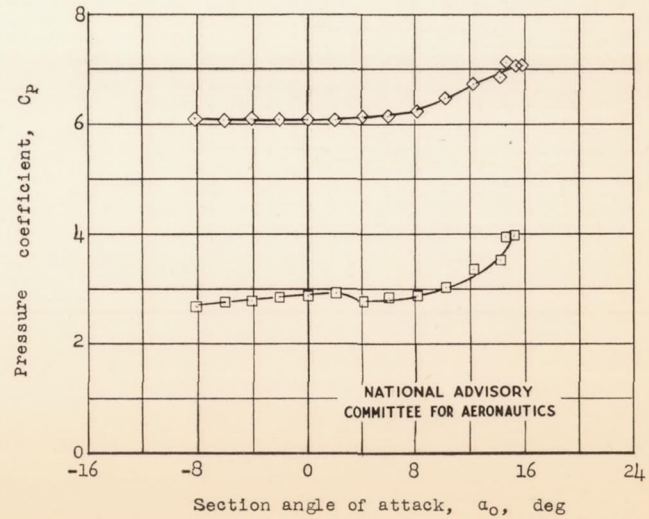

(b) $R = 6.0 \times 10^6$; model in smooth condition.

Figure 5.- Continued.

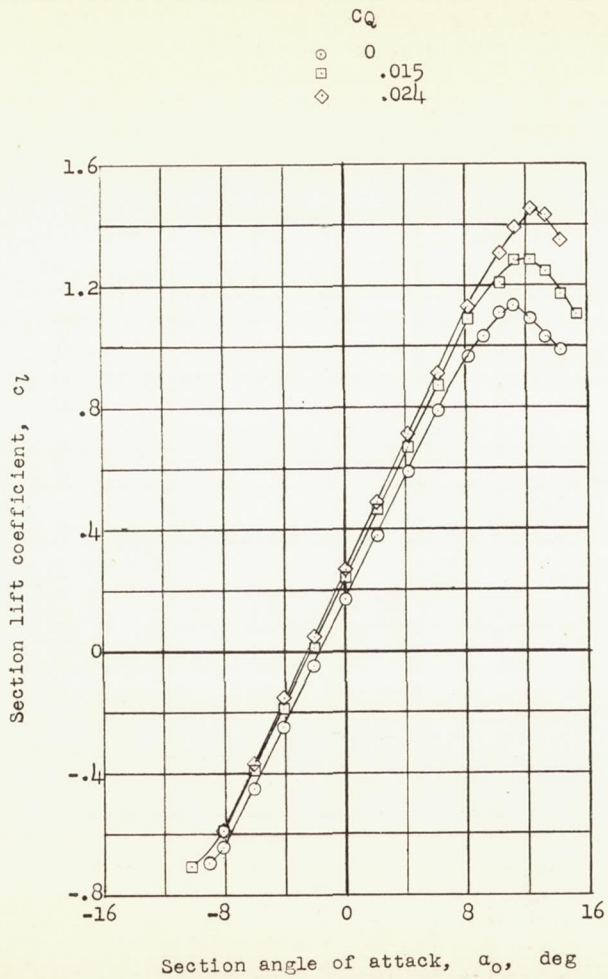

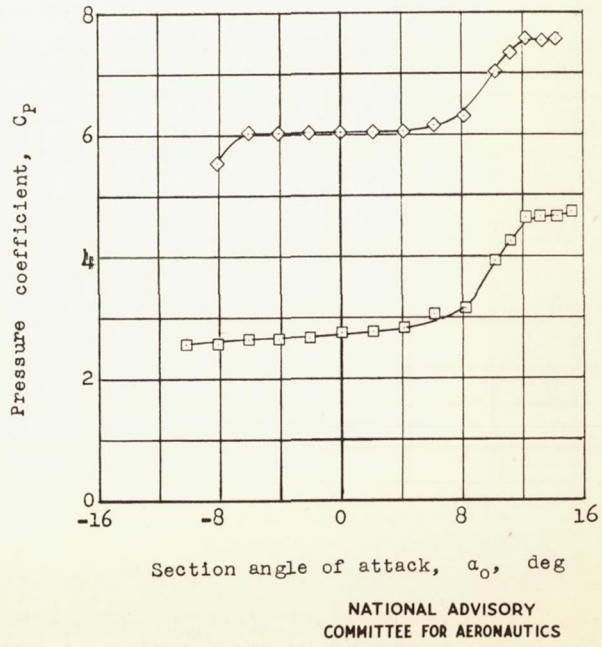

(c) $R = 6.0 \times 10^6$; model with standard roughness.

Figure 5.- Concluded.

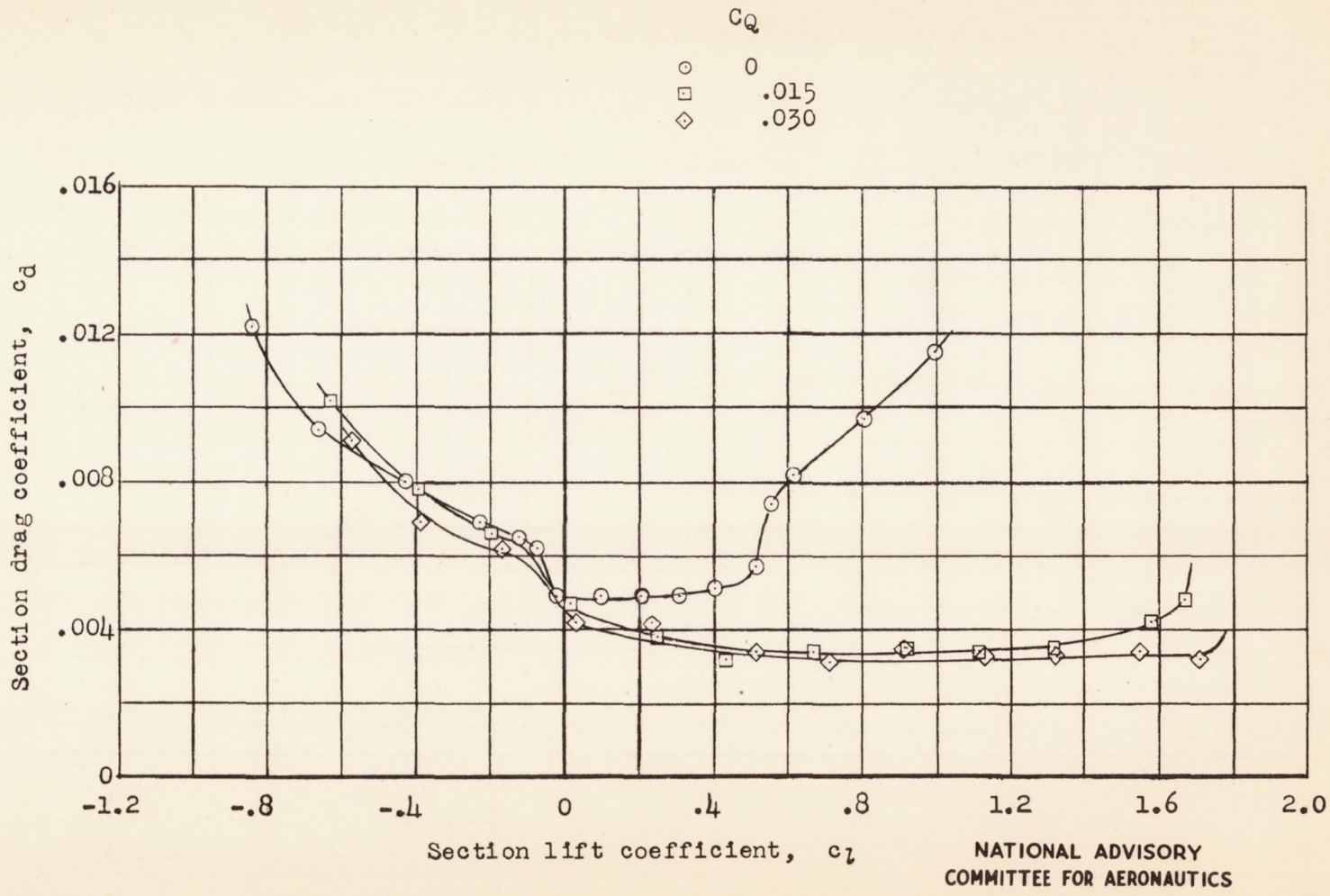

(a) $R = 3.0 \times 10^6$; model in smooth condition.

Figure 6.- Drag characteristics of NACA 64_1A212 airfoil section with boundary-layer control. Tests, TDT 953, 984.

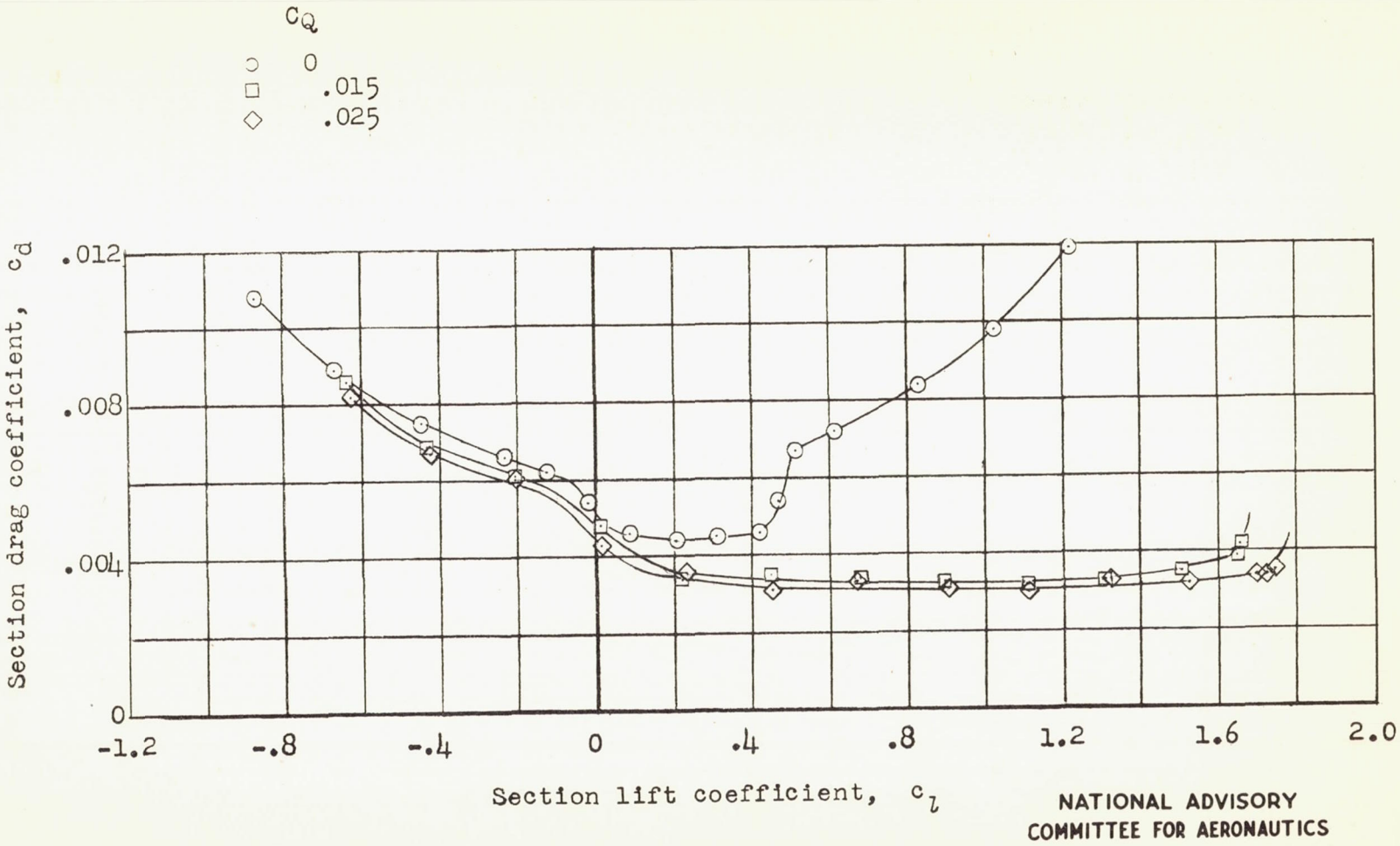

(b) $R = 6.0 \times 10^6$; model in smooth condition.

Figure 6.- Continued.

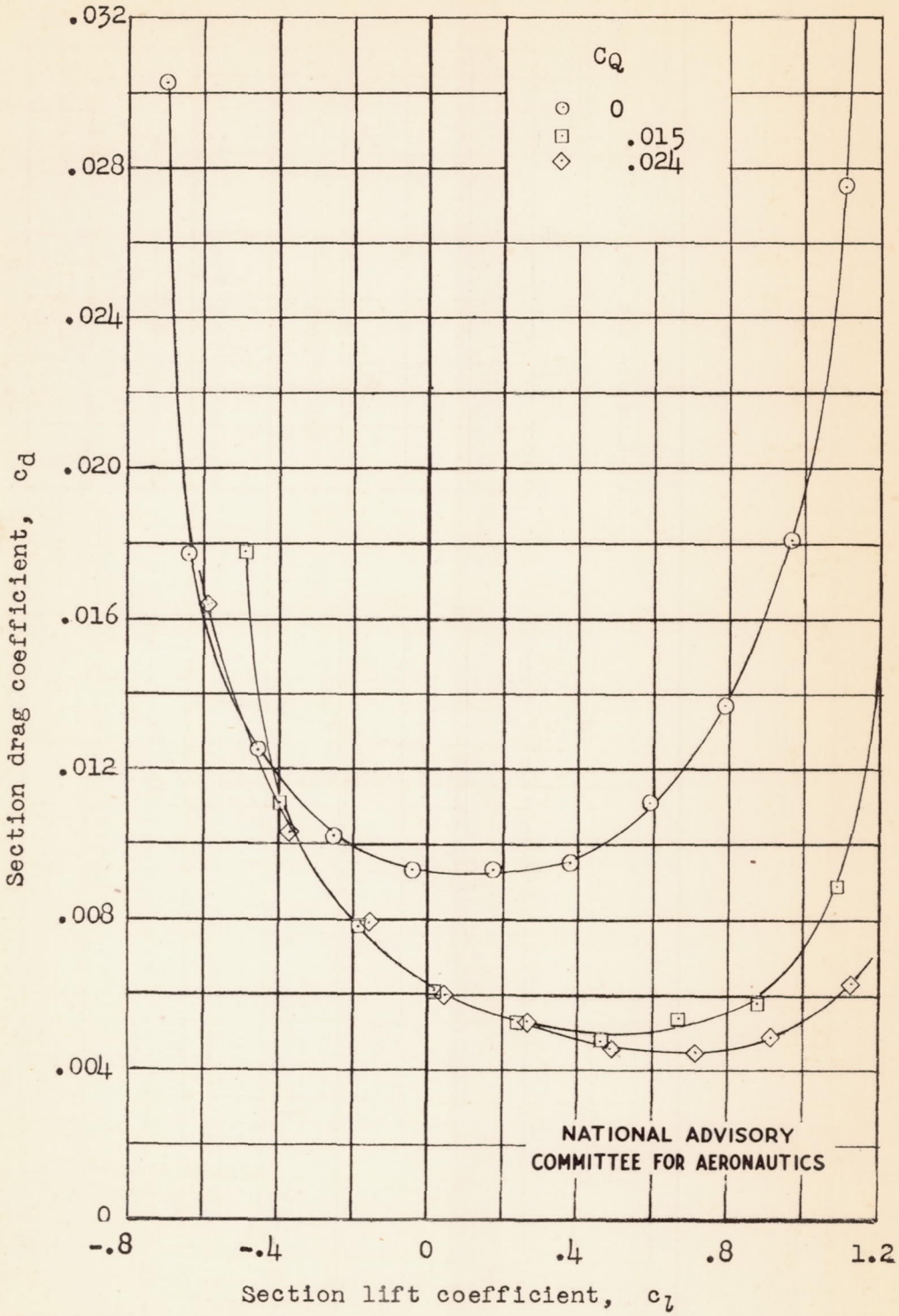

(c) $R = 6.0 \times 10^6$; model with standard roughness.

Figure 6.- Concluded.

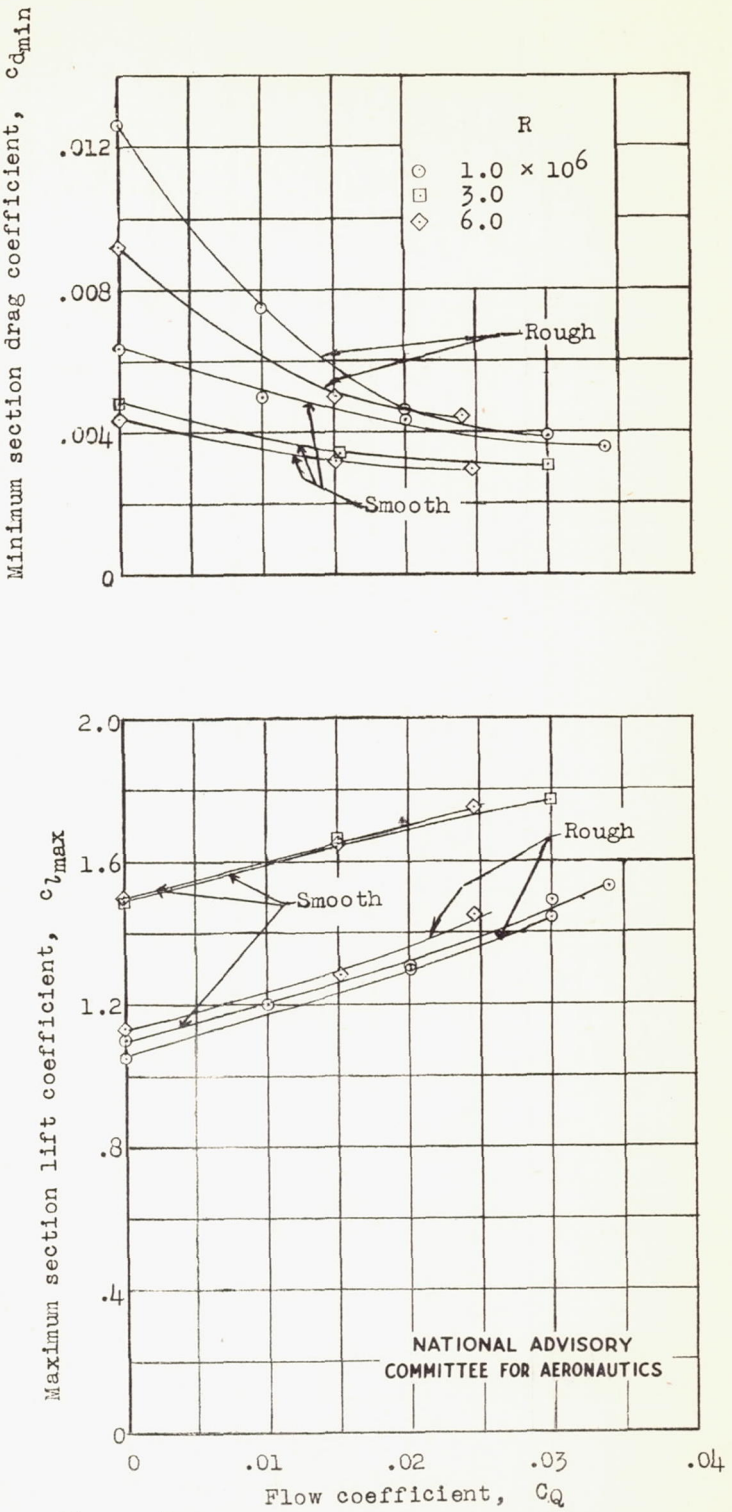

Figure 7.- Effect of Reynolds number and leading-edge roughness on variation of maximum section lift coefficient and minimum section drag coefficient with flow coefficient for NACA 64_1A212 airfoil section.

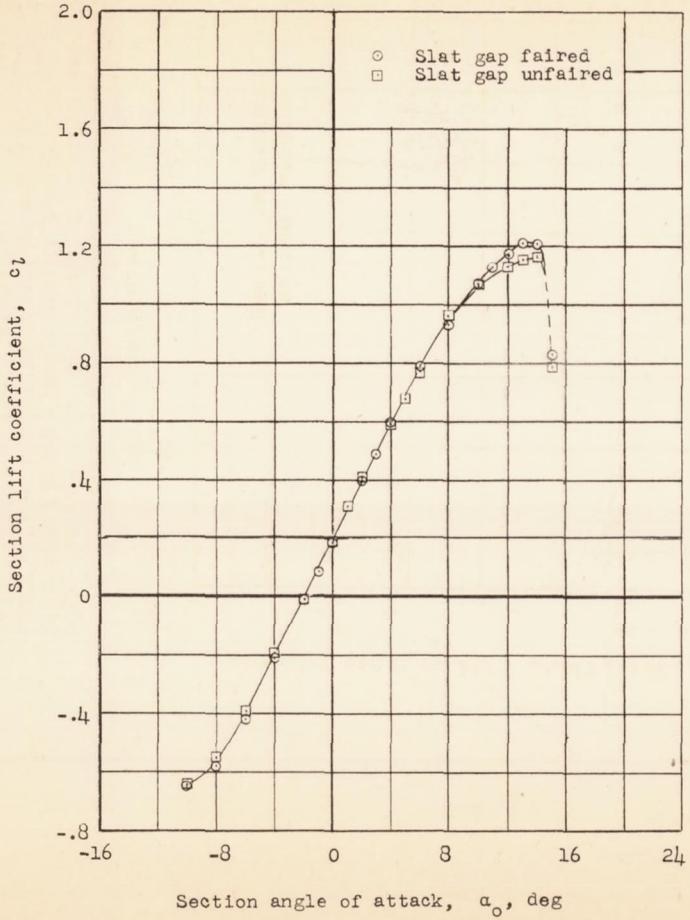

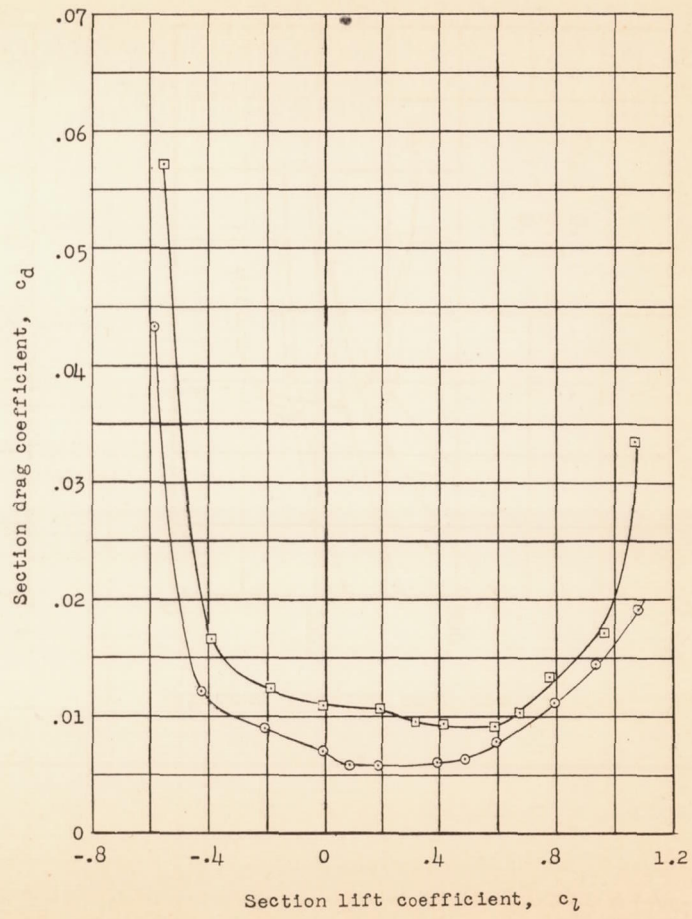

NATIONAL ADVISORY
COMMITTEE FOR AERONAUTICS

Figure 8.- Effect of rounding slat leading edge on lift and drag characteristics of NACA 64_1A212 airfoil section with slat retracted. C_Q, 0; R, 1.5×10^6; test, LTT 437.

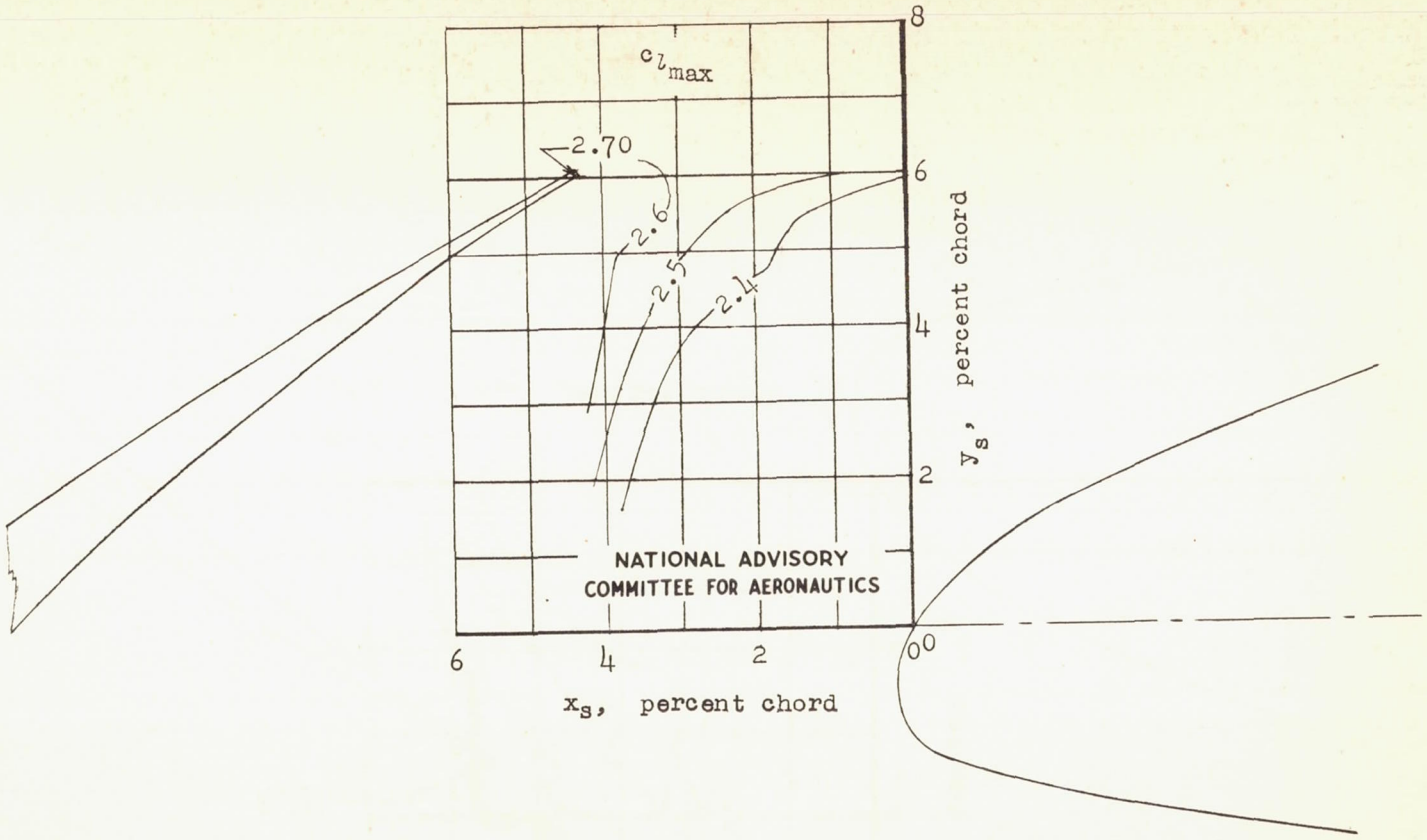

(a) $\delta_s = 18.2^\circ$.

Figure 9 .- Leading-edge-slat maximum-lift contours for various slat deflections on NACA 64_1A212 airfoil section. R, 1.0×10^6; C_Q, 0.03 (approx.); flap retracted; test, LTT 437.

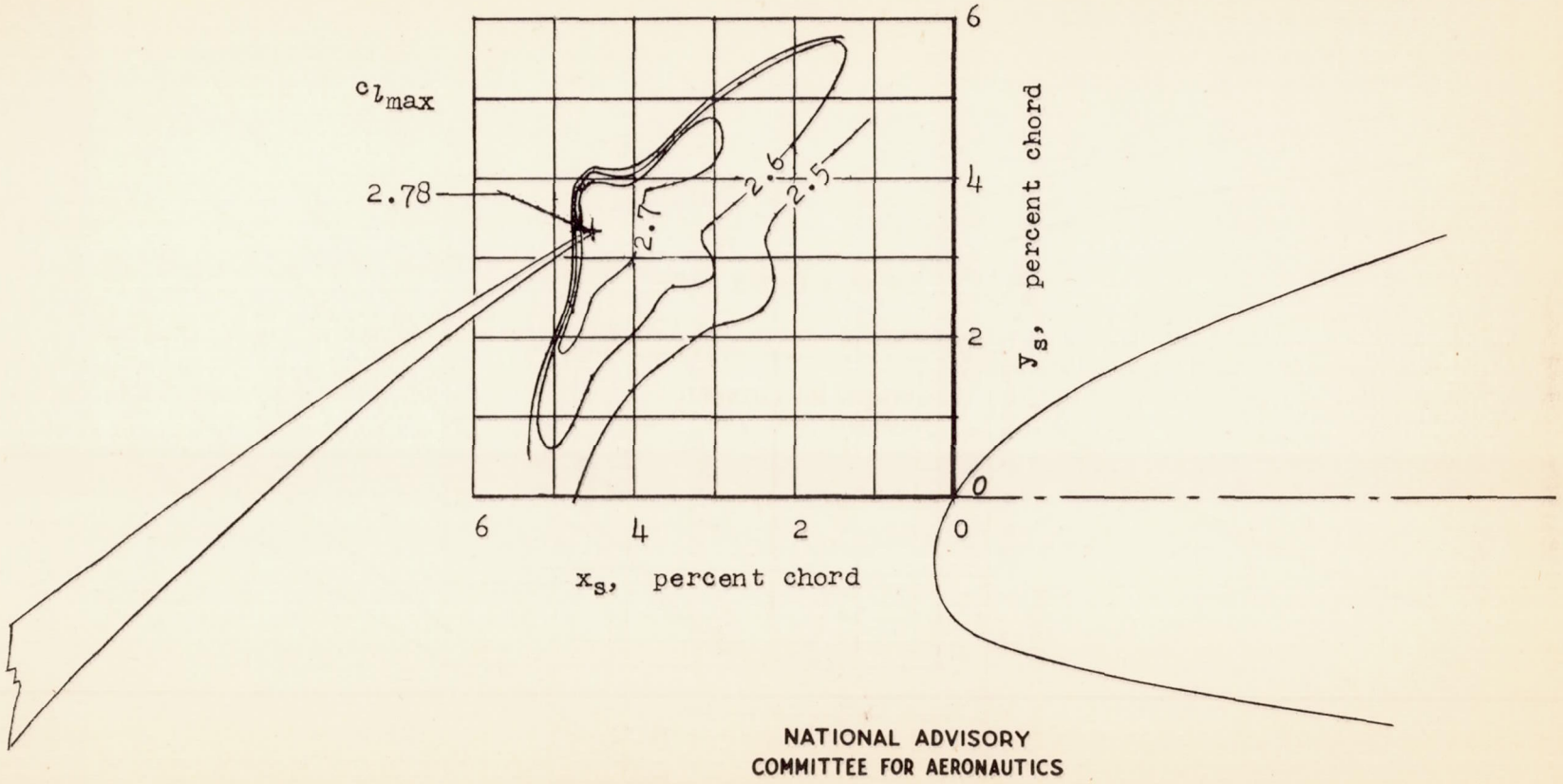

(b) $\delta_s = 22.0^\circ$.

Figure 9.- Continued.

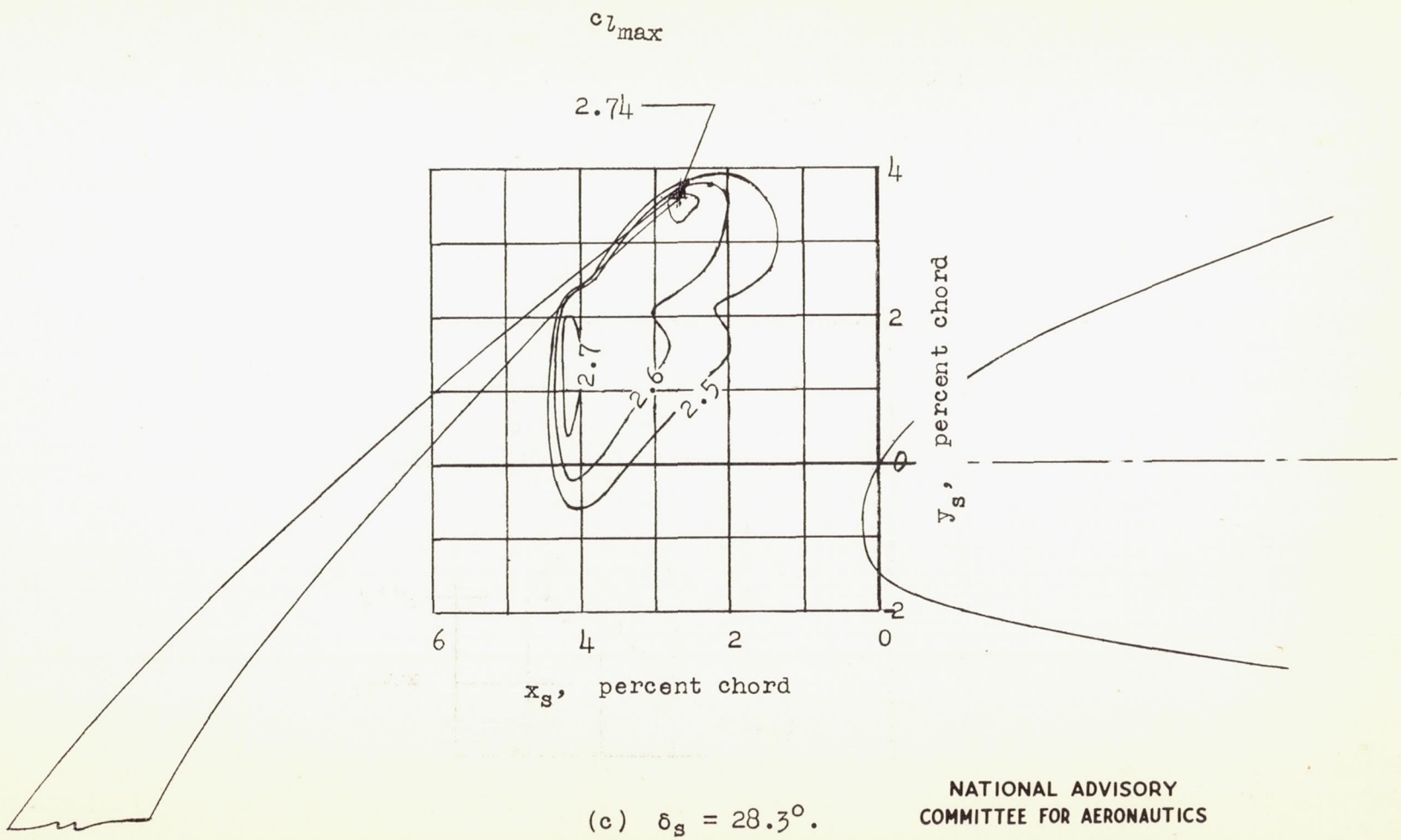

NATIONAL ADVISORY
COMMITTEE FOR AERONAUTICS

(c) $\delta_s = 28.3°$.

Figure 9.- Concluded.

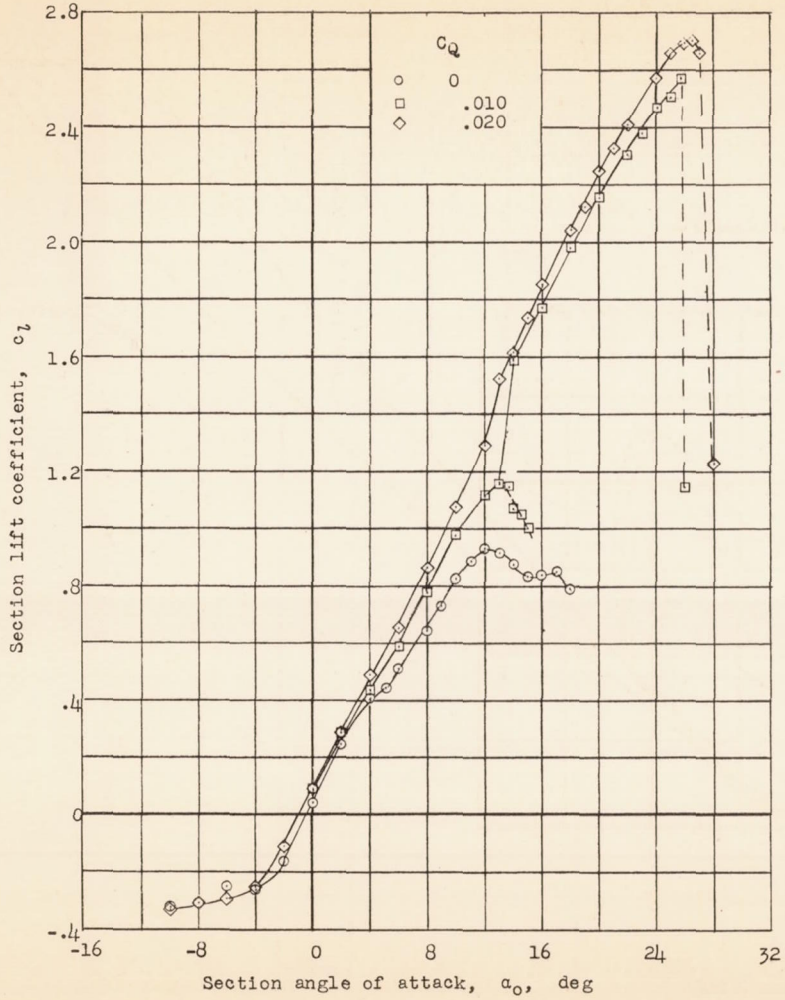

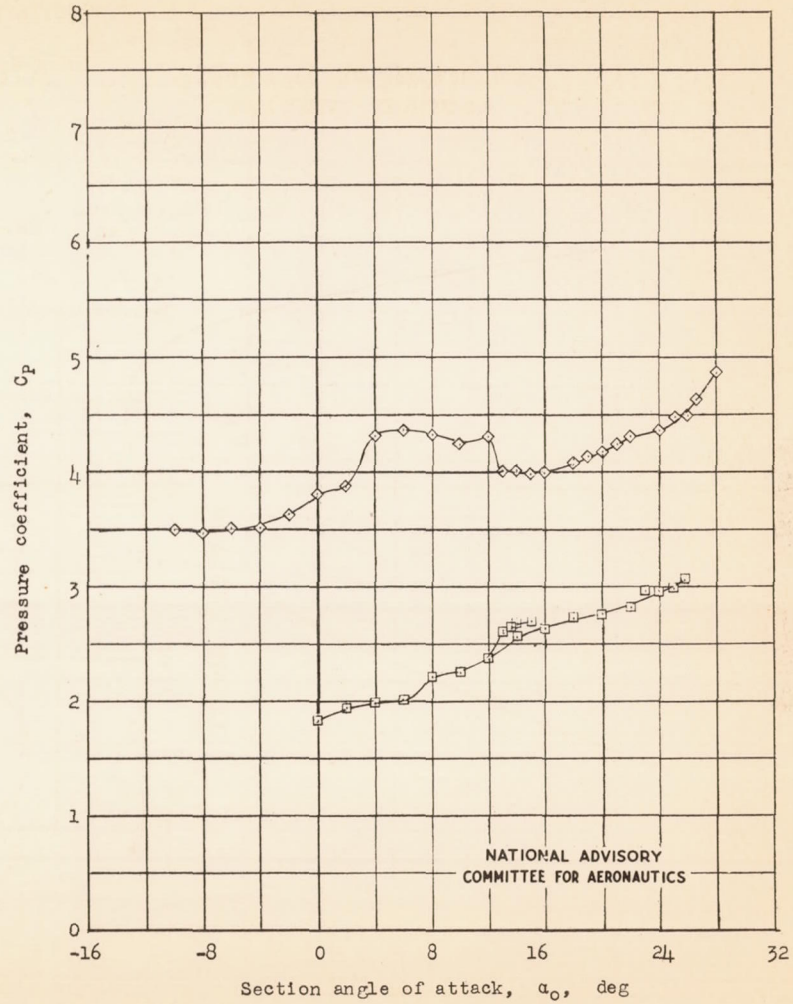

(a) Lift characteristics; $R = 1.5 \times 10^6$.

Figure 10.- Aerodynamic characteristics of NACA 64_1A212 airfoil section with leading-edge slat and boundary-layer control. δ_s, 22.0°; x_s, 0.046c; y_s, 0.037c; flap retracted; test, LTT 437.

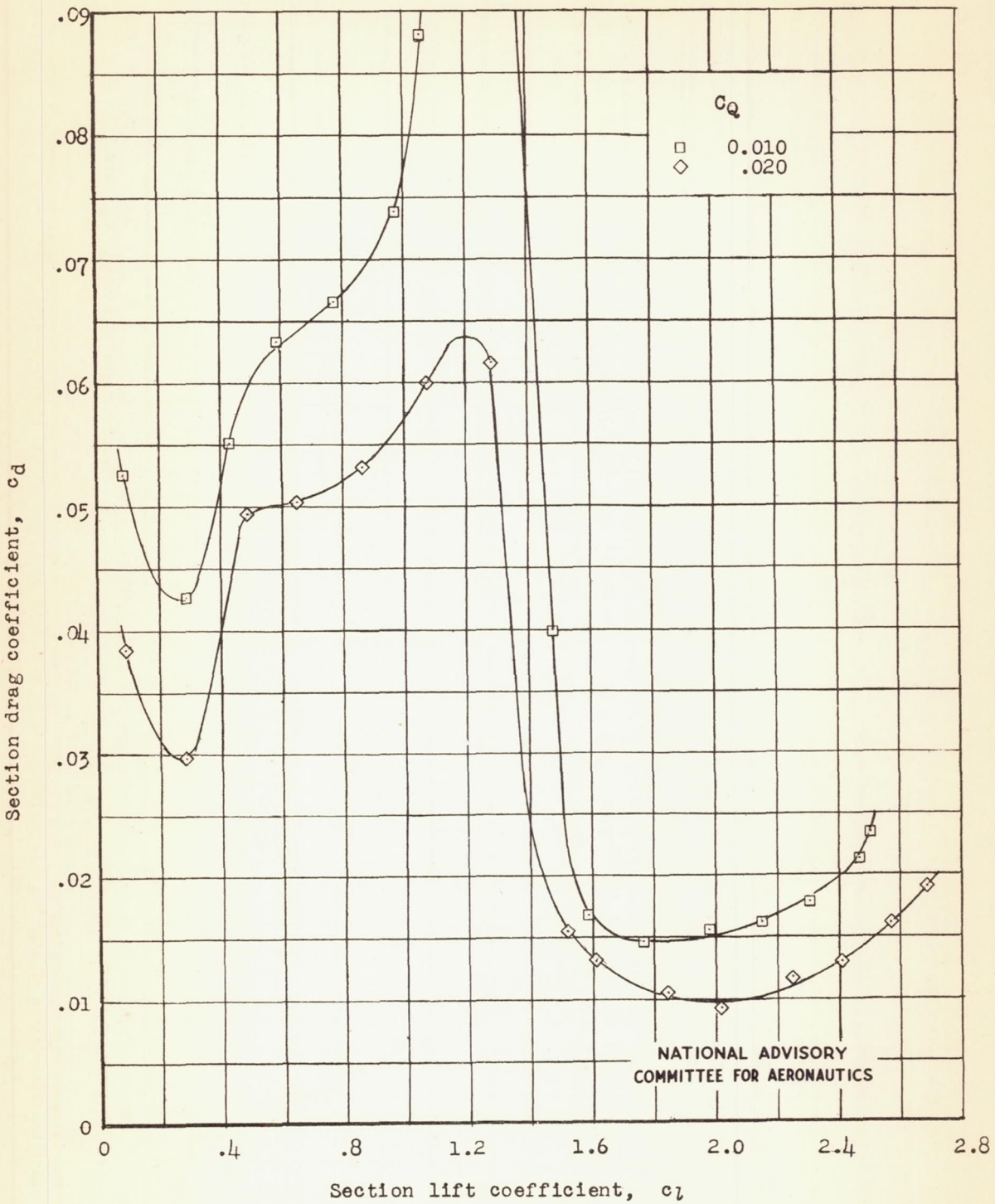

(b) Drag characteristics; $R = 1.5 \times 10^6$.

Figure 10.- Concluded.

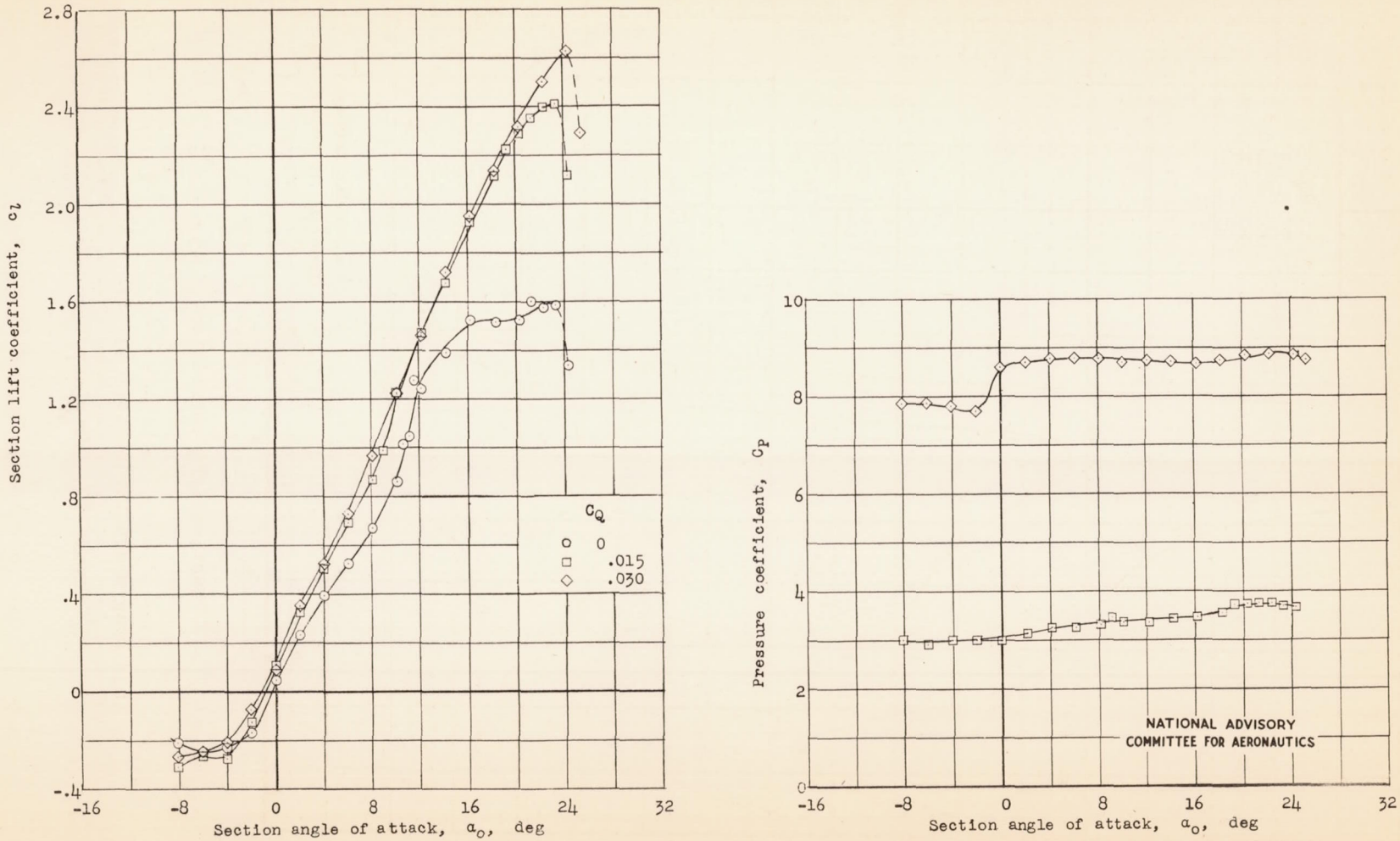

(a) $R = 1.5 \times 10^6$; model in smooth condition.

Figure 11.- Lift characteristics of NACA 64_1A212 airfoil section with leading-edge slat and boundary-layer control. δ_s, 22.0°; x_s, 0.036c; y_s, 0.037c; flap retracted; test, TDT 990.

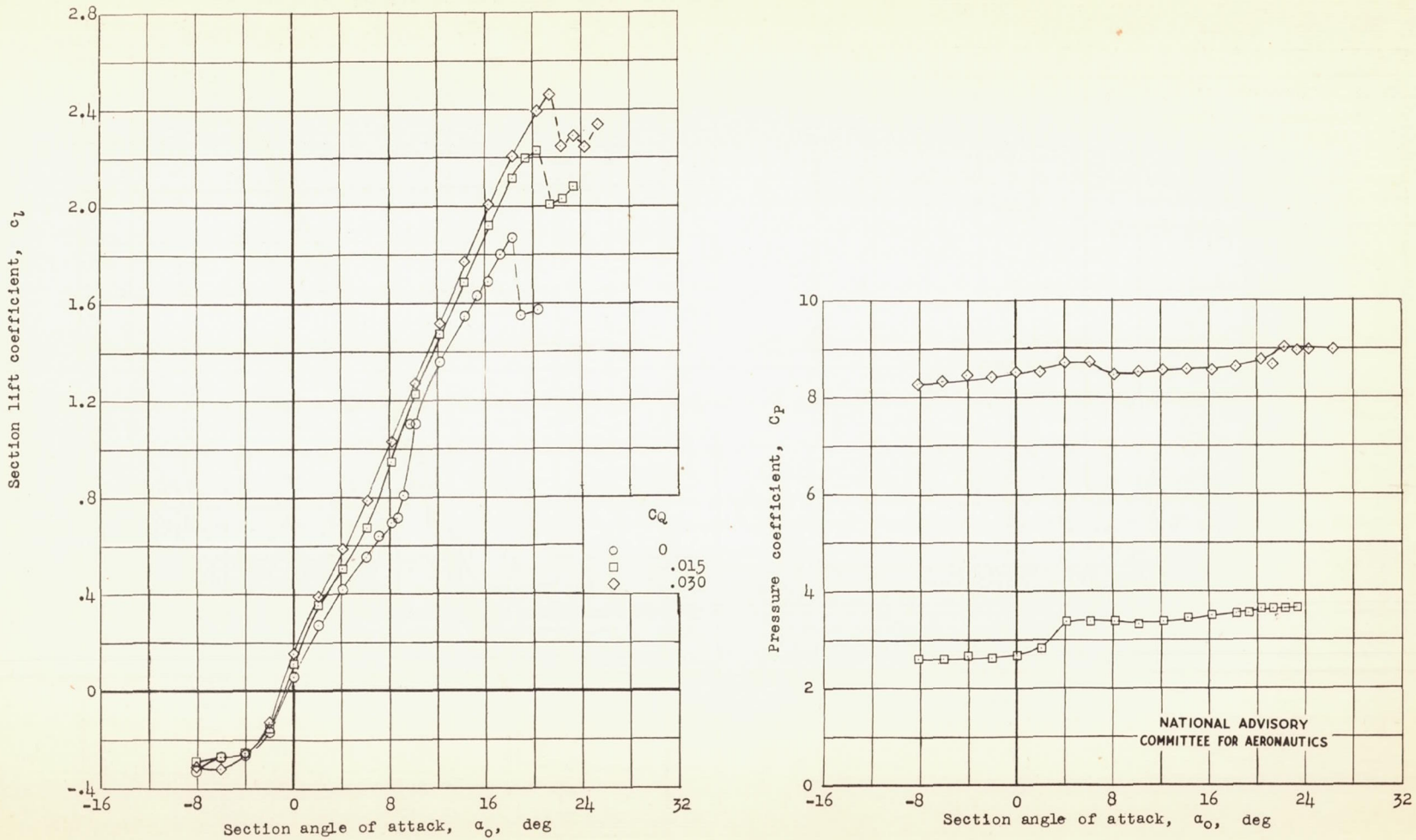

(b) $R = 3 \times 10^6$; model in smooth condition.

Figure 11.- Continued.

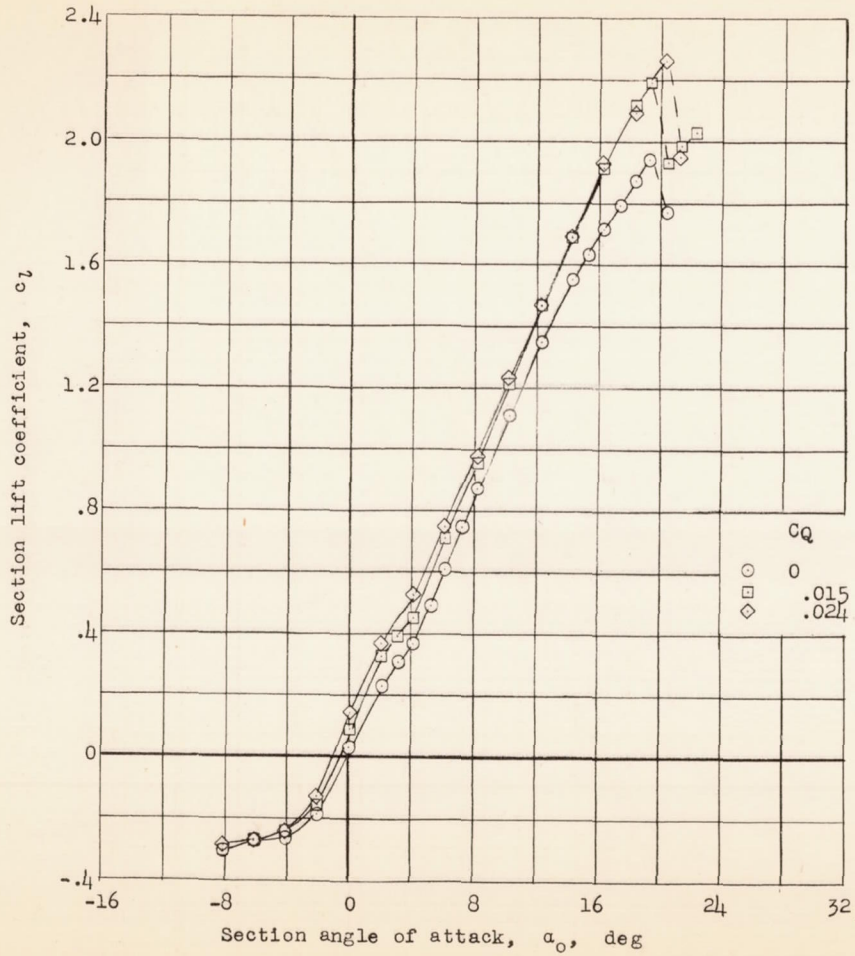

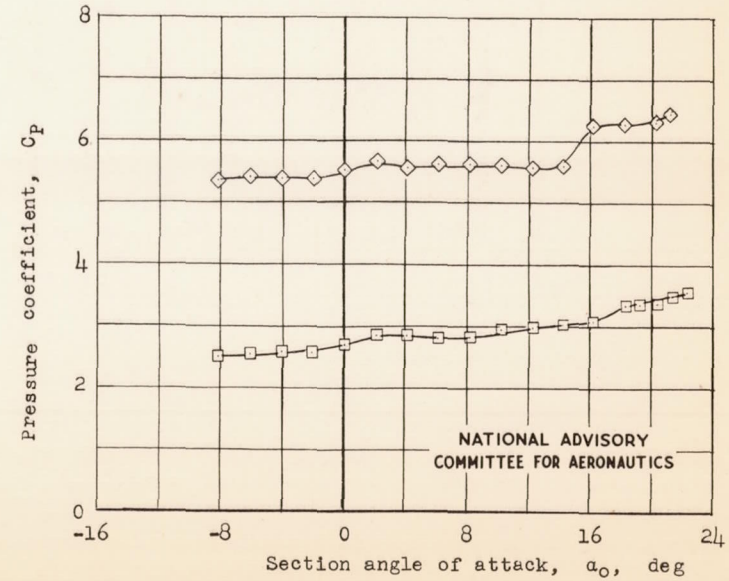

(c) $R = 6 \times 10^6$; model in smooth condition.

Figure 11.- Continued.

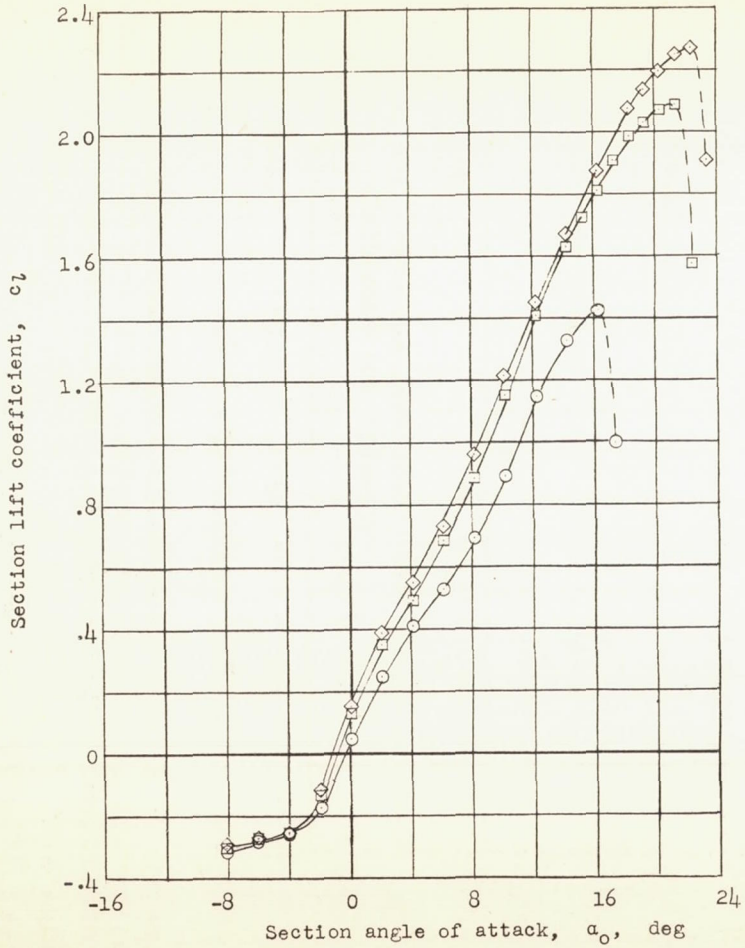

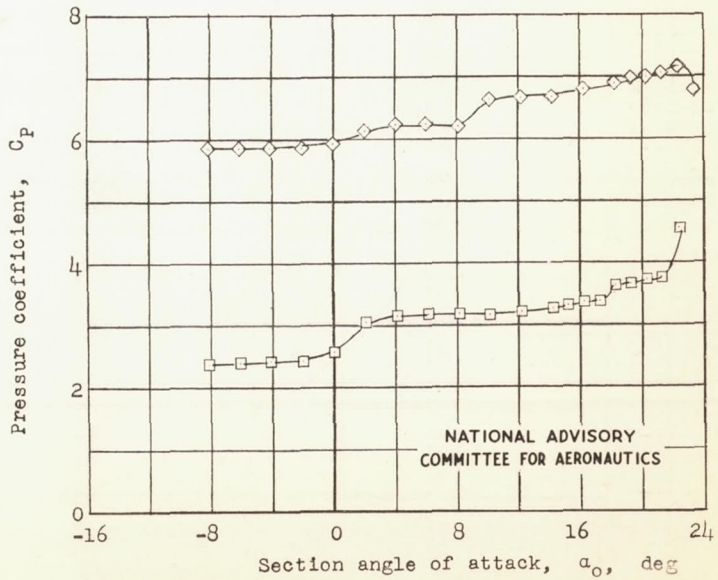

(d) $R = 6 \times 10^6$; model with standard roughness.

Figure 11.- Concluded.

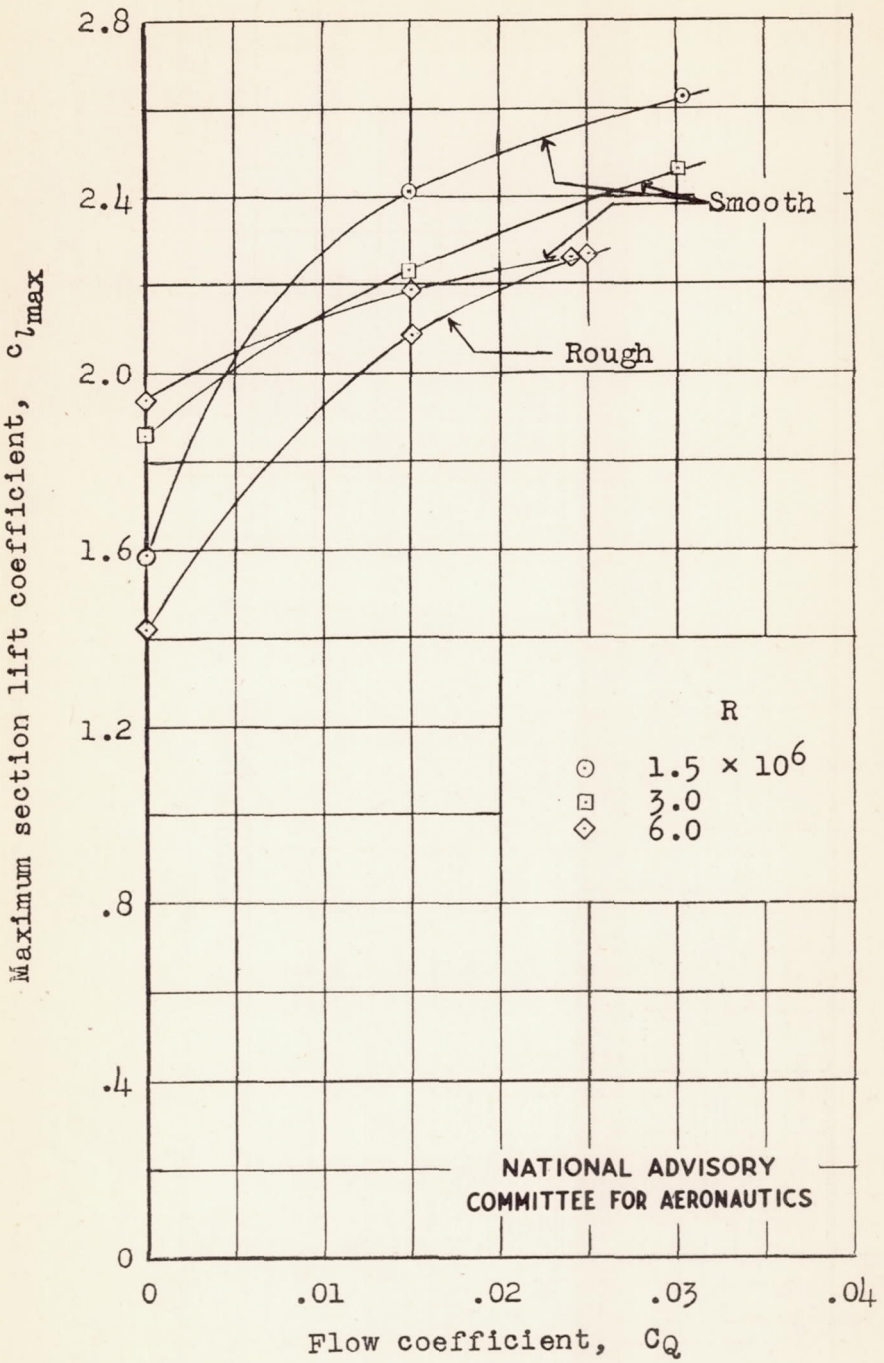

Figure 12.- Effect of Reynolds number and leading-edge roughness on variation of maximum section lift coefficient with flow coefficient for NACA 64_1A212 airfoil section with leading-edge slat. δ_s, 22.0°; x_s, 0.036c; y_s, 0.037c; test, TDT 990.

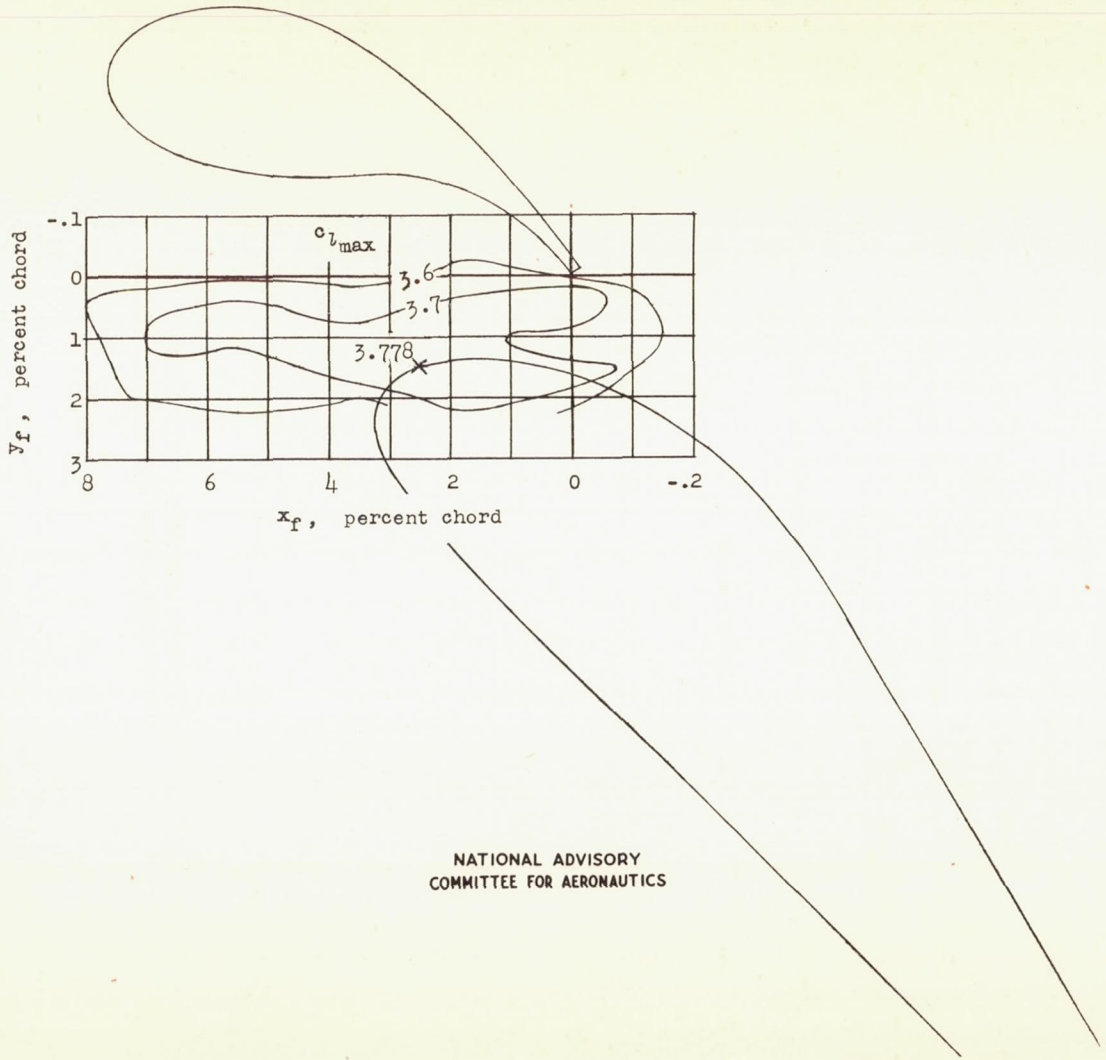

(a) Positions of flap with respect to vane; δ_f, 49.7°; x_v, 0.009c; y_v, 0.020c.

Figure 13.- Double-slotted-flap maximum lift contours on NACA 64_1A212 airfoil section. x_s, 0.036; y_s, 0.037c; δ_s, 22.0°; δ_v, 16.5°; R, 1.5×10^6; C_Q, 0.02 (approx.); test, LTT 437.

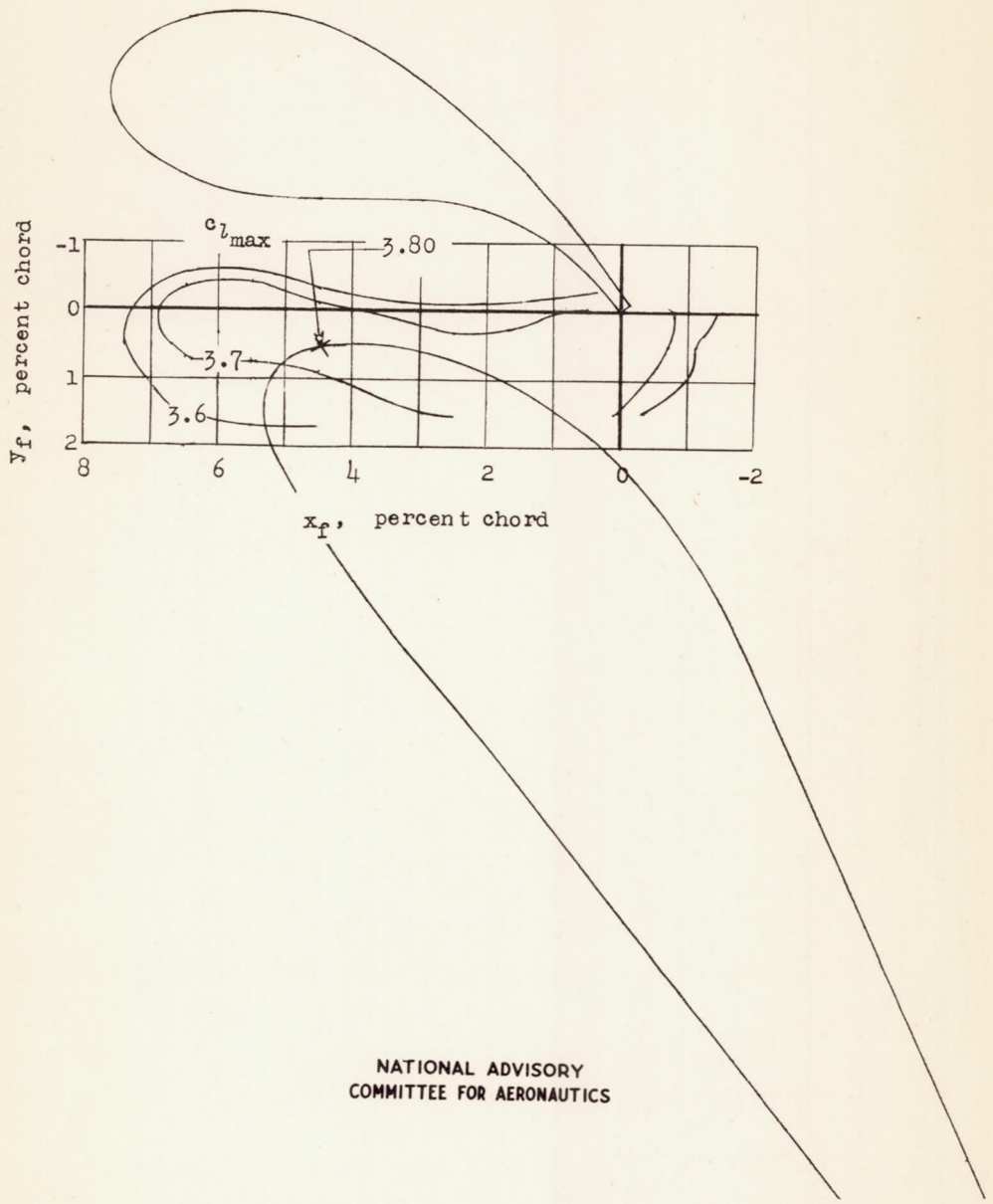

(b) Positions of flap with respect to vane. δ_f, 55.0°; x_v, 0.009c; y_v, 0.020c.

Figure 13.- Continued.

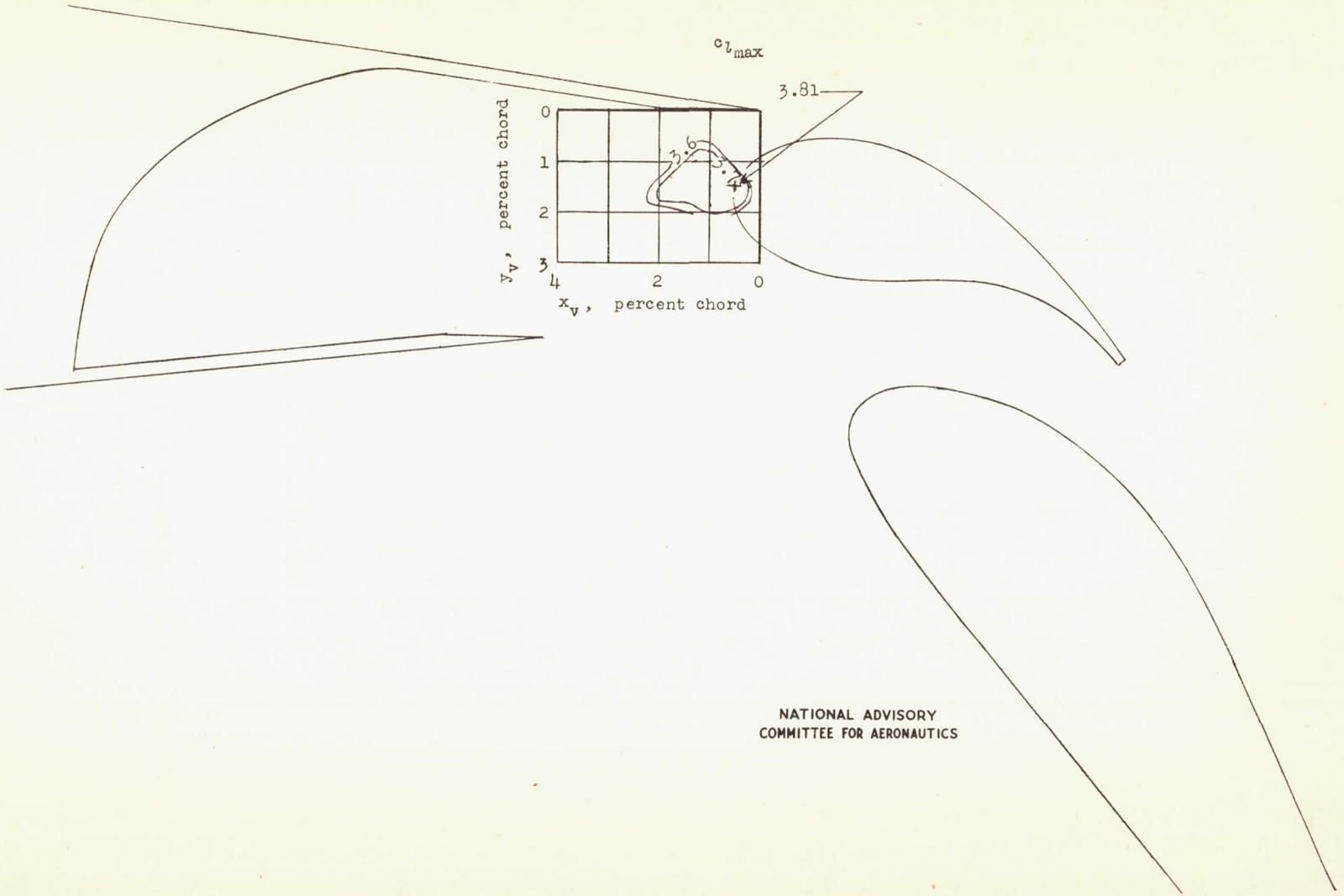

(c) Positions of double slotted flap with respect to wing; δ_f, 55.0°; x_f, 0.044c; y_f, 0.005c.

Figure 13.- Concluded.

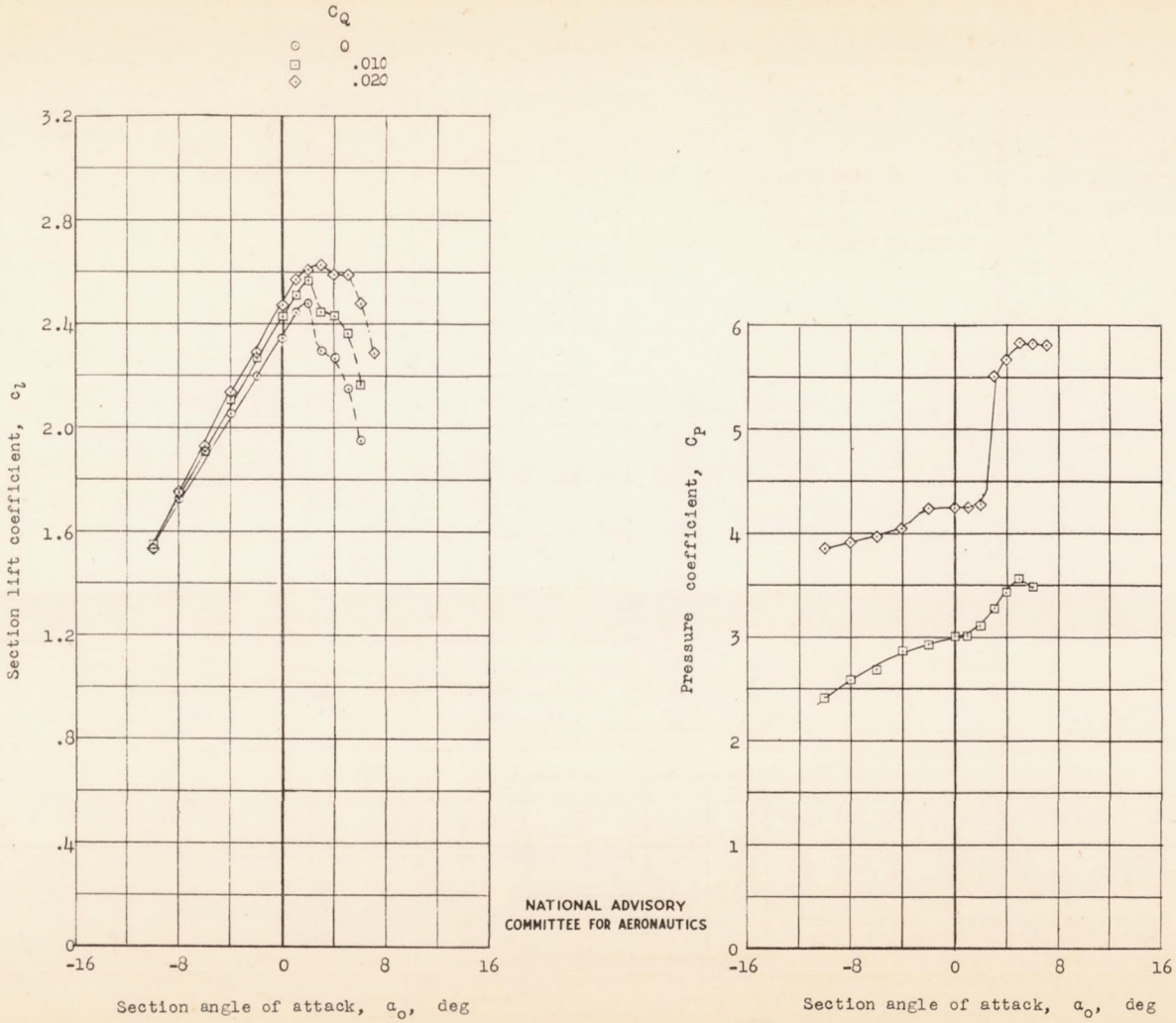

(a) $R = 1.5 \times 10^6$; model in smooth condition; test, LTT 437.

Figure 14.- Lift characteristics of NACA 64_1A212 airfoil section with double slotted flap and boundary-layer control. δ_v, 16.5°; x_v, 0.004c; y_v, 0.014c; δ_f, 55.0°; x_f, 0.044c; y_f, 0.005c.

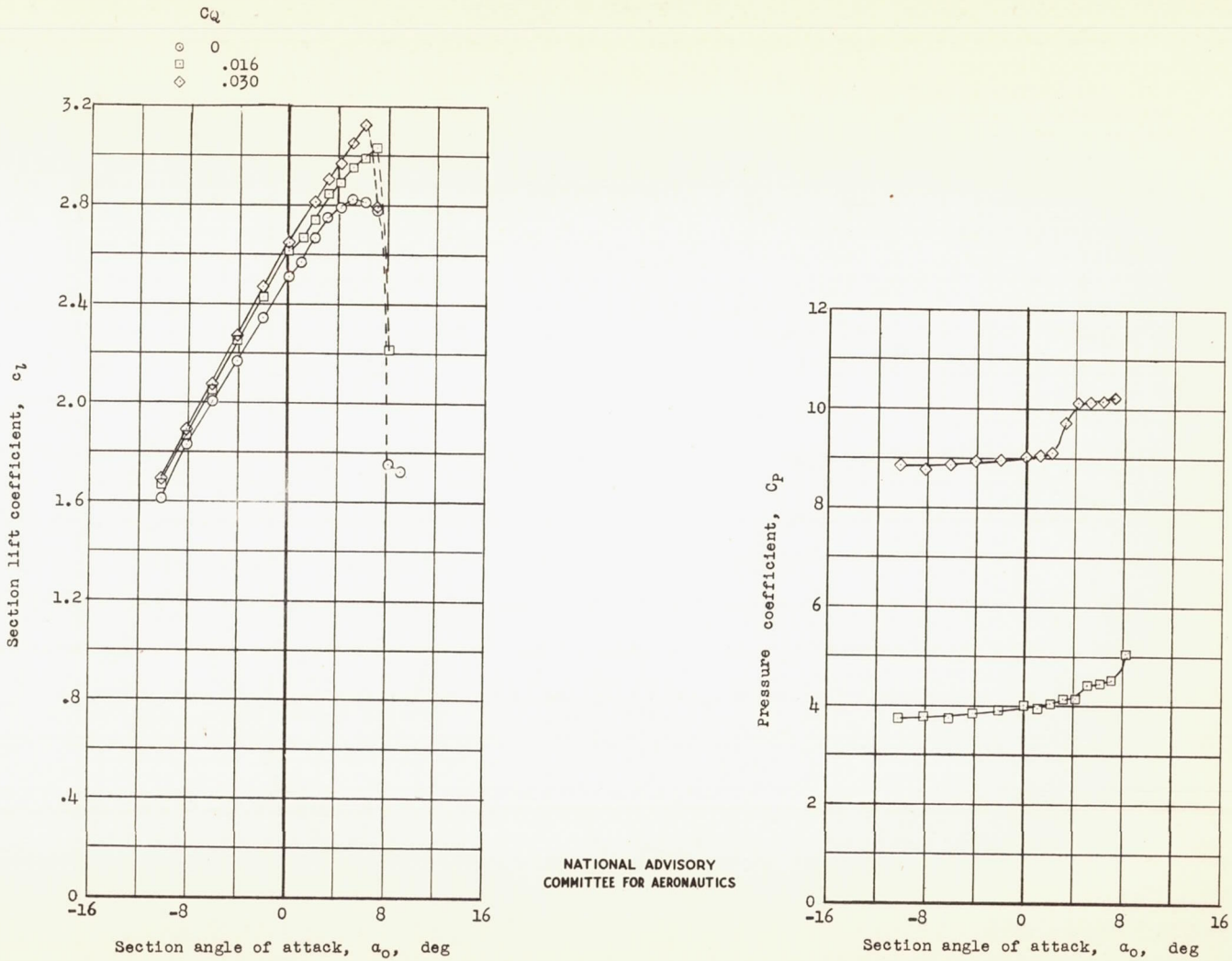

(b) $R = 3.0 \times 10^6$; model in smooth condition; test, TDT 984.

Figure 14.- Continued.

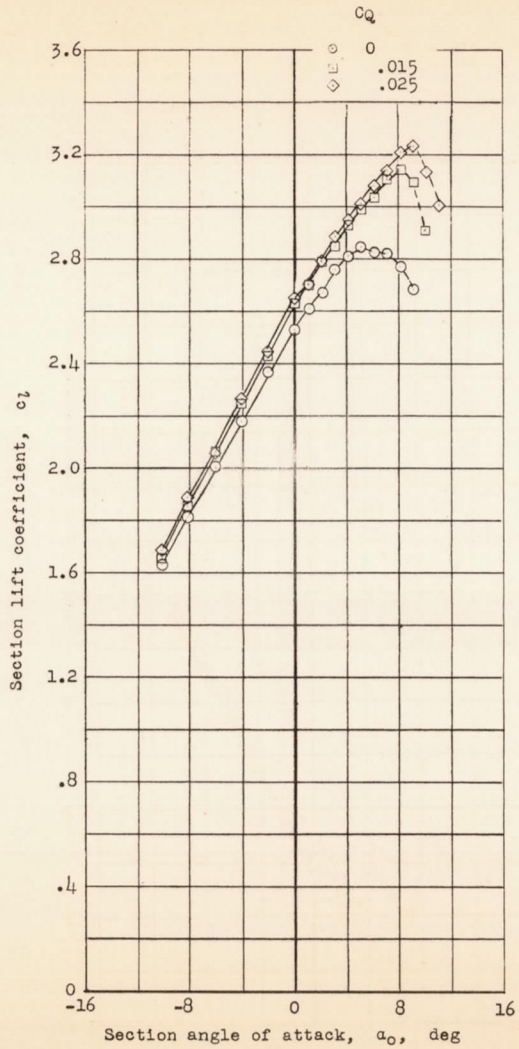

NATIONAL ADVISORY
COMMITTEE FOR AERONAUTICS

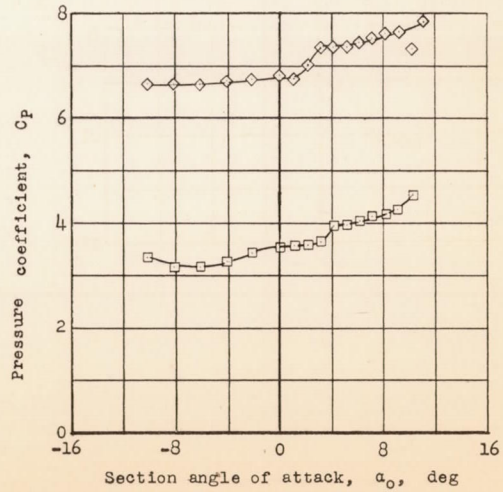

(c) $R = 6.0 \times 10^6$; model in smooth condition; test, TDT 984.

Figure 14.- Continued.

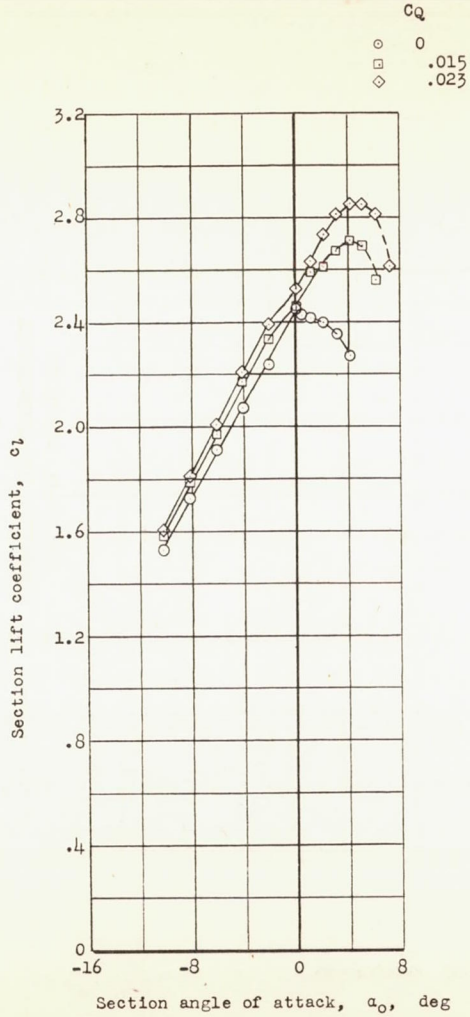

NATIONAL ADVISORY
COMMITTEE FOR AERONAUTICS

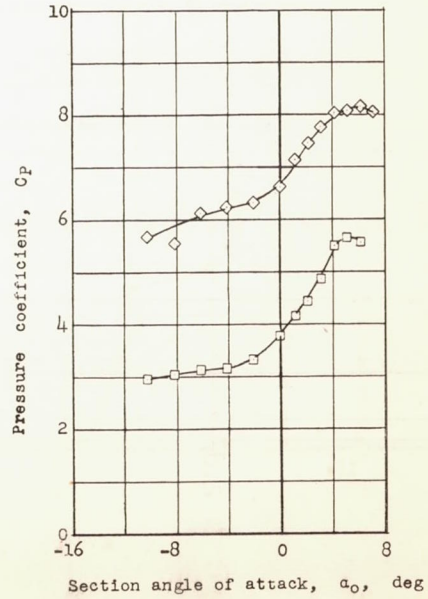

(d) $R = 6.0 \times 10^6$; model with standard roughness; test, TDT 984.

Figure 14.- Concluded.

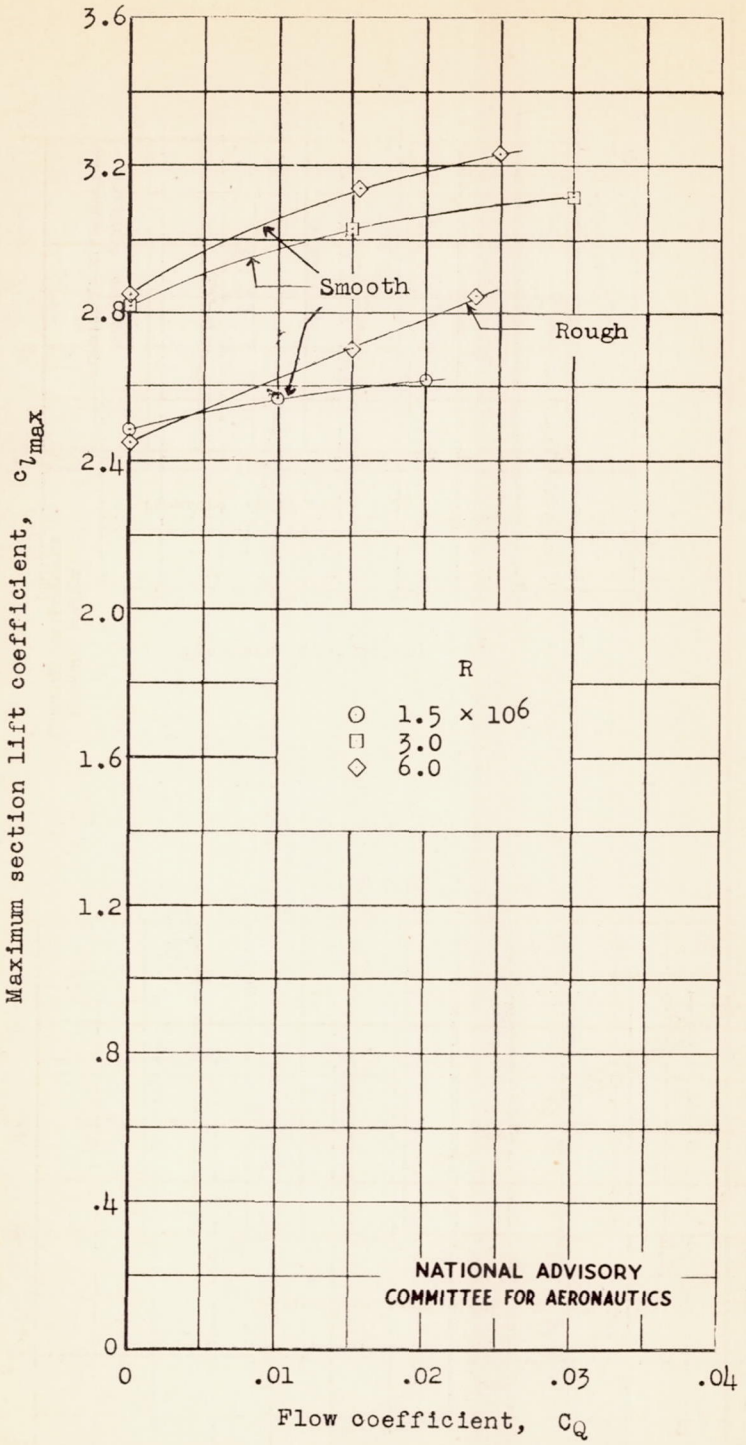

Figure 15.- Effect of Reynolds number and leading-edge roughness on variation of maximum section lift coefficient with flow coefficient for NACA 64_1A212 airfoil section with double slotted flap. δ_v, 16.5°; x_v, 0.004c; y_v, 0.014c; δ_f, 55.0°; x_f, 0.044c; y_f, 0.005c; test, TDT 990.

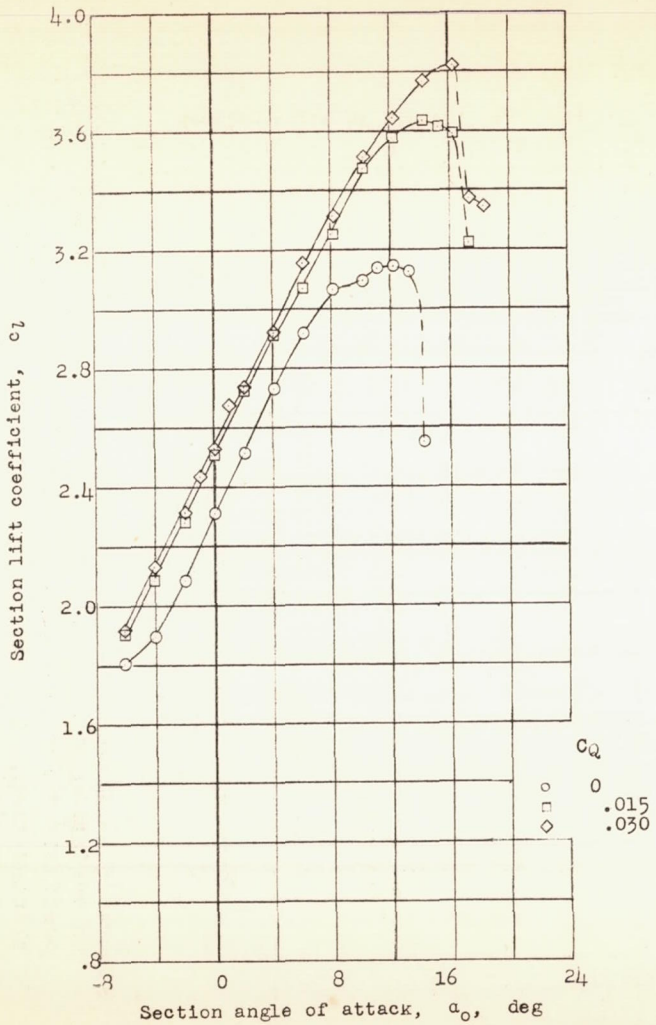

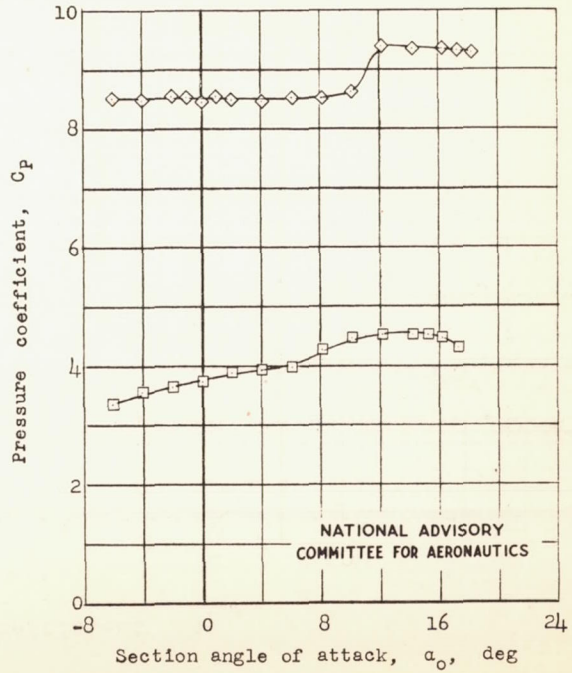

(a) $R = 1.5 \times 10^6$; model in smooth condition.

Figure 16.- Lift characteristics of NACA 64_1A212 airfoil section with leading-edge slat, double slotted flap, and boundary-layer control. δ_s, 22.0°; x_s, 0.036c; y_s, 0.037c; δ_v, 16.5°; x_v, 0.004c; y_v, 0.014c; δ_f, 55.0°; x_f, 0.044c; y_f, 0.005c; test, TDT 990.

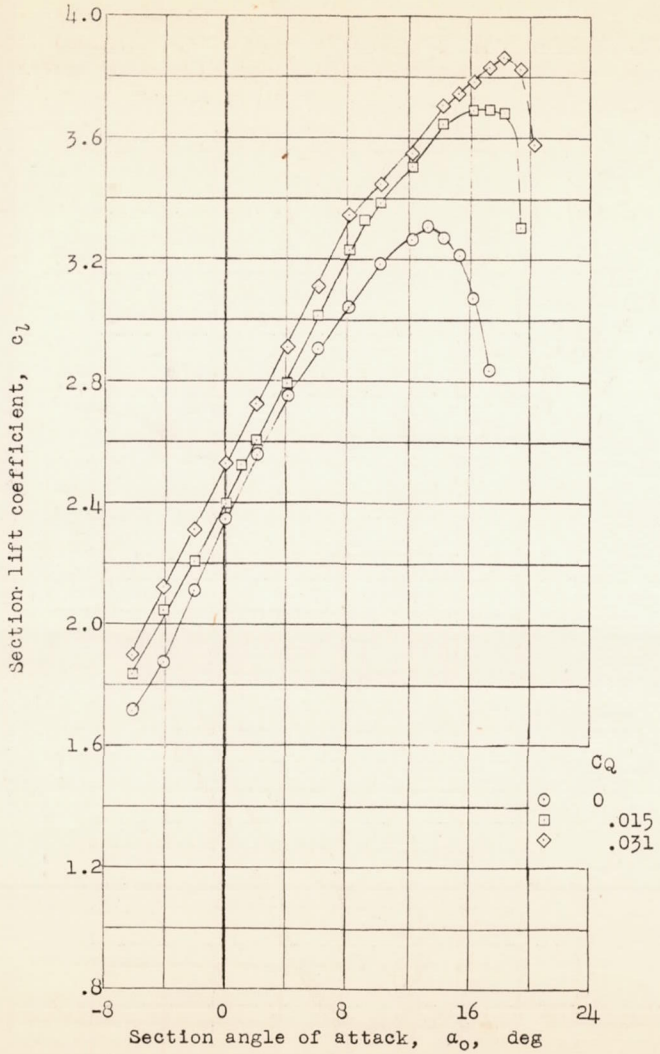

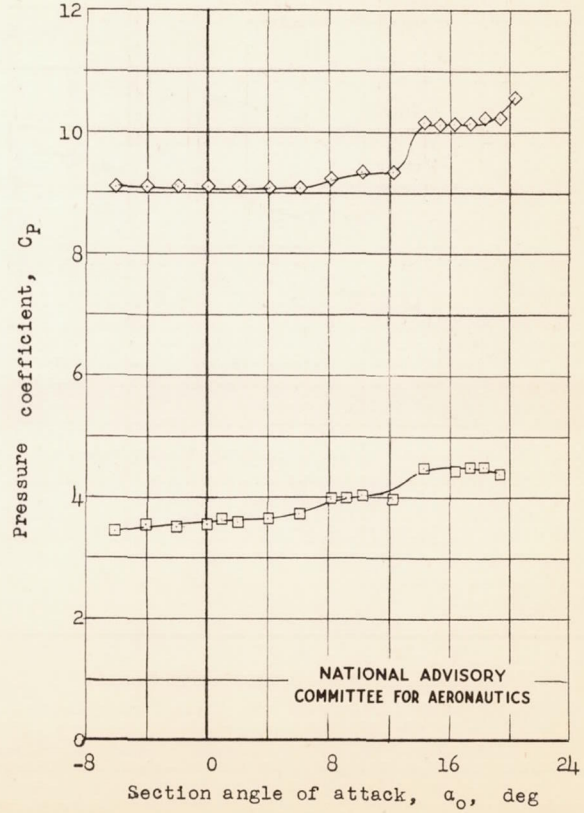

(b) $R = 3 \times 10^6$; model in smooth condition.

Figure 16.- Continued.

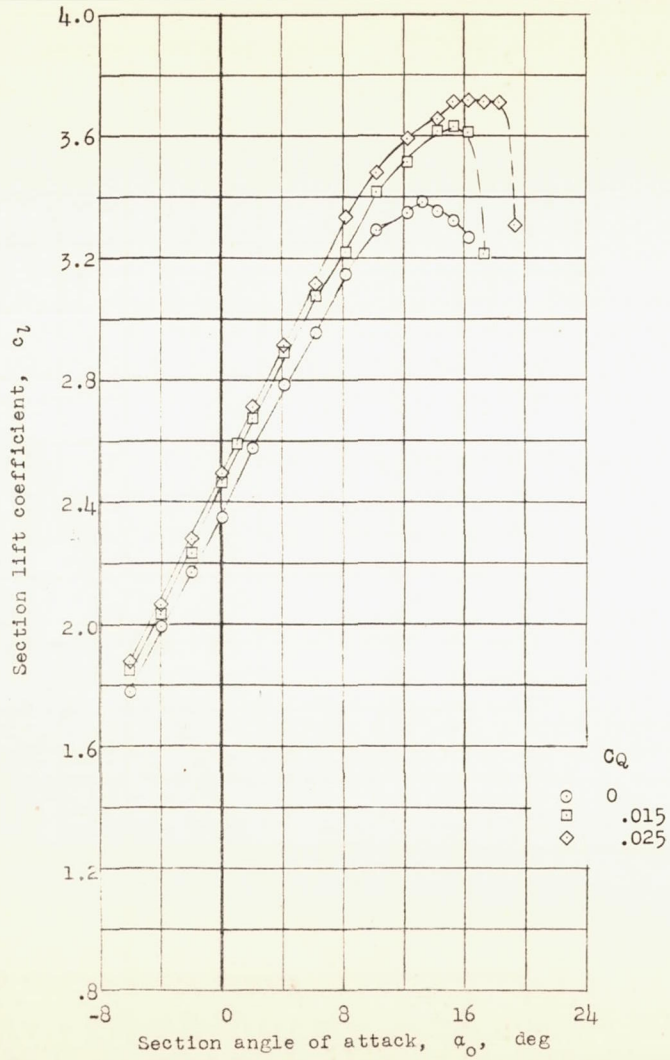

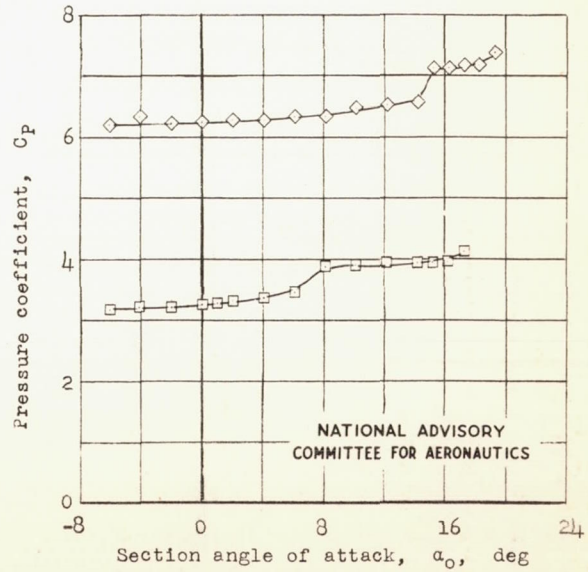

(c) R = 6.0×10^6; model in smooth condition.

Figure 16.- Continued.

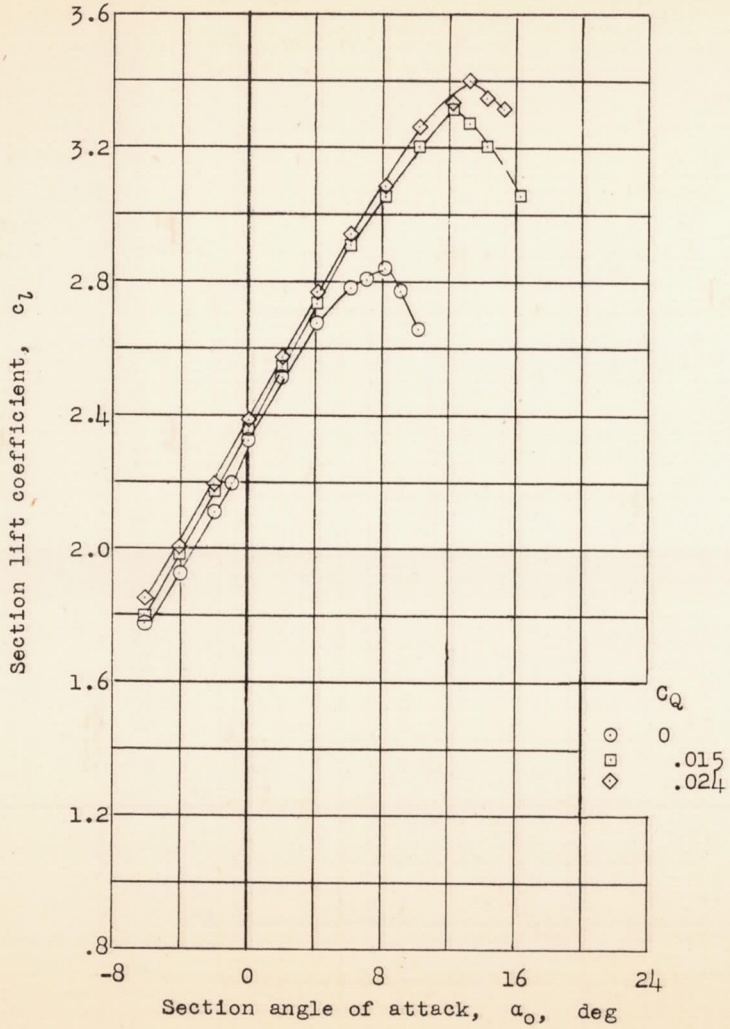

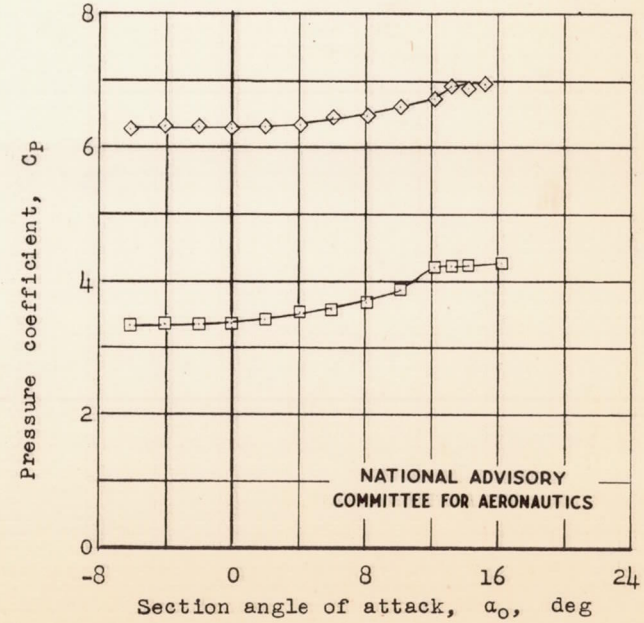

(d) $R = 6.0 \times 10^6$; model with standard roughness.

Figure 16.- Concluded.

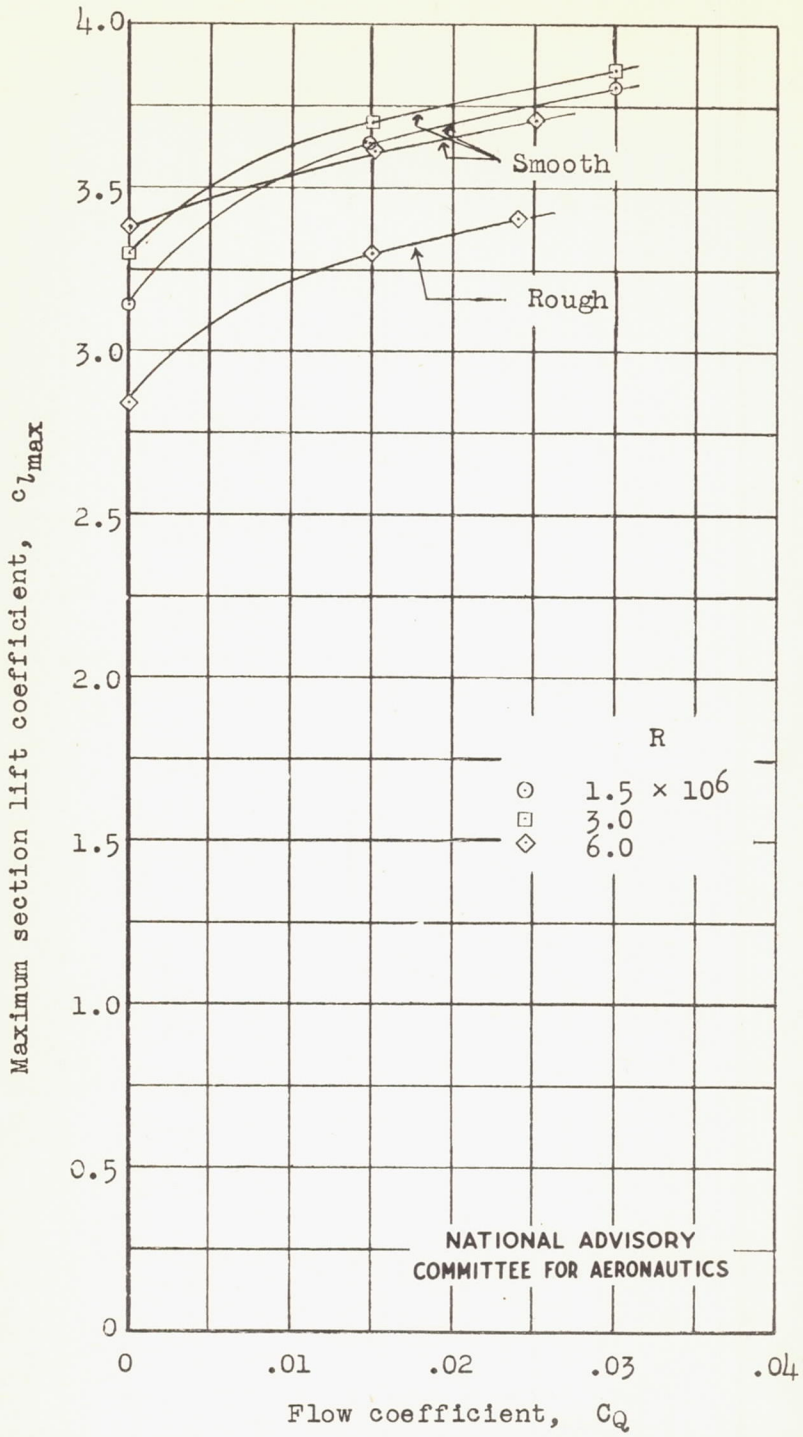

Figure 17.- Effect of Reynolds number and leading-edge roughness on variation of maximum section lift coefficient with flow coefficient for NACA 64_1A212 airfoil section with leading-edge slat and double slotted flap. δ_s, 22.0°; x_s, 0.036c; y_s, 0.037c; δ_v, 16.5°; x_v, 0.004c; y_v, 0.014c; δ_f, 55.0°; x_f, 0.044c; y_f, 0.005c; test, TDT 990.